Tuning Low-Adiabat Cryogenic Implosions on OMEGA

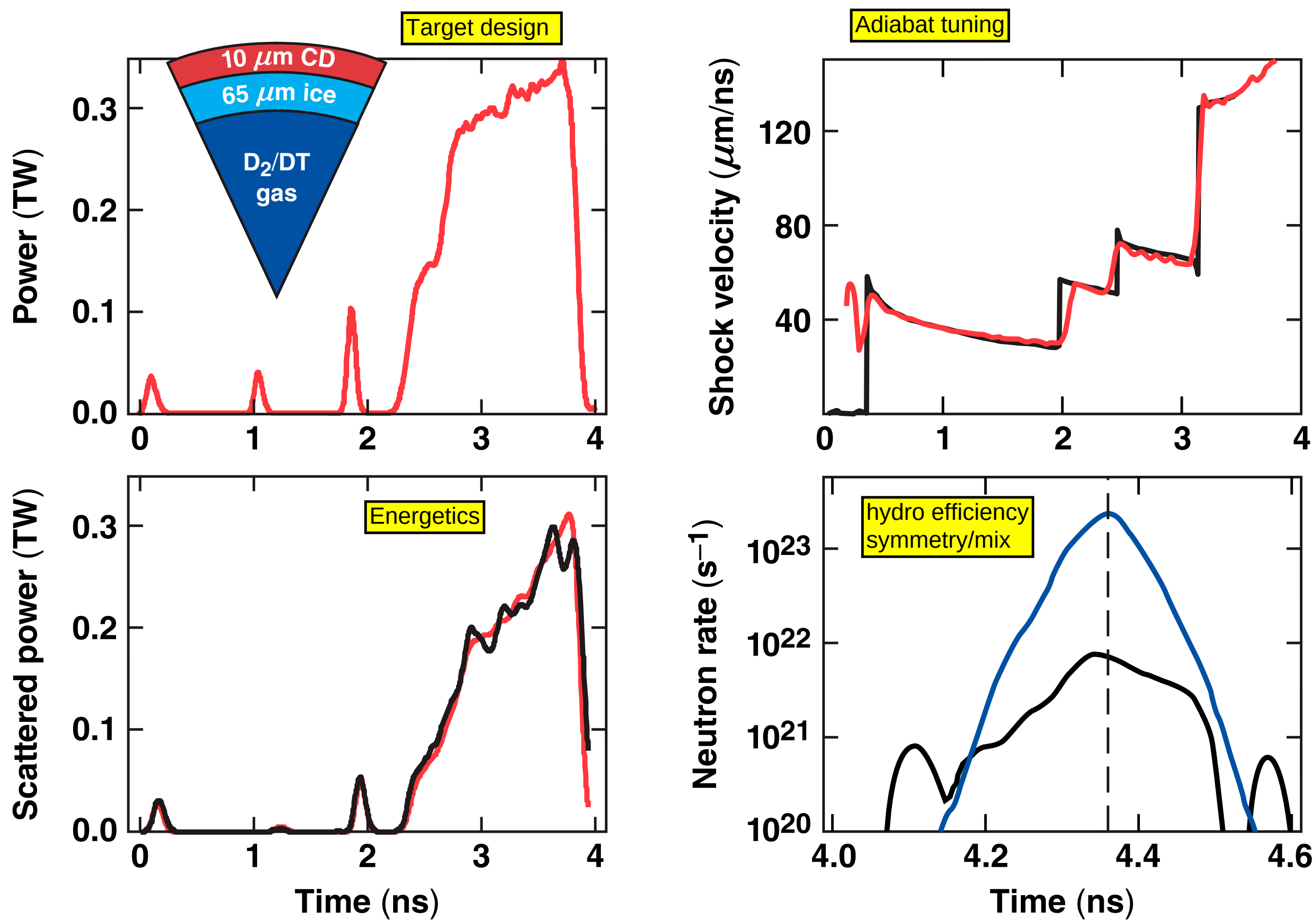

V. N. Goncharov
University of Rochester
Laboratory for Laser Energetics

Omega Laser Facility
Users' Group Workshop
Rochester, NY
27–29 April 2011

Summary

Modeling of cryogenic implosions on OMEGA is approaching precision required for ignition

- The majority of the observables are consistent with calculations when the nonlocal thermal transport is used and the effect of cross-beam energy transfer is taken into account in the laser-deposition modeling
- Areal densities measured in cryogenic implosions are in agreement with 1-D predictions
- At current levels of nonuniformity sources (offset, ice roughness, condensables, ablator finish), measured ion temperature is lower than 1-D calculation by ~20% and yield is ~5% to 10% of 1-D predictions
- With improved nonuniformity, cryogenic implosions on OMEGA are predicted to achieve YOC ~15% to 20% with $\langle T_i \rangle$ ~90%$\langle T_i \rangle_{1\text{-D}}$

Ignition condition depends on fuel areal density, ion temperature, and yield

- Minimum shell kinetic energy required for ignition[1]

$$E \sim V^{-6}\alpha^4 \qquad \alpha = \frac{P}{P_{\mathrm{Fermi}}}$$

- Threshold factor[2]—measured conditions at neutron-production time

$$\chi = \langle \rho R \rangle^{0.8} \left(\frac{\langle T_{\mathrm{i}} \rangle}{4.7\ \mathrm{keV}} \right)^{1.6} \mathrm{YOC}^{0.5} \qquad \chi > 1 \text{ required for ignition}$$

One of the main goals of the cryogenic campaign on OMEGA is to validate modeling of $\langle \rho R \rangle$, $\langle T_{\mathrm{i}} \rangle$, and yield.

[1] S. Haan *et al.*, "Point Design Targets, Specifications, and Requirements for the 2010 Ignition Campaign on the National Ignition Facility," submitted to Phys. Plasmas

[2] R. Betti *et al.*, Phys. Plasmas 17, 058102 (2010).

Low-adiabat cryogenic implosions on OMEGA are driven using $\alpha = 2.0$ and $\alpha = 2.5$ target designs

$\alpha = 2.5$
$E_L = 22$ to 23 kJ

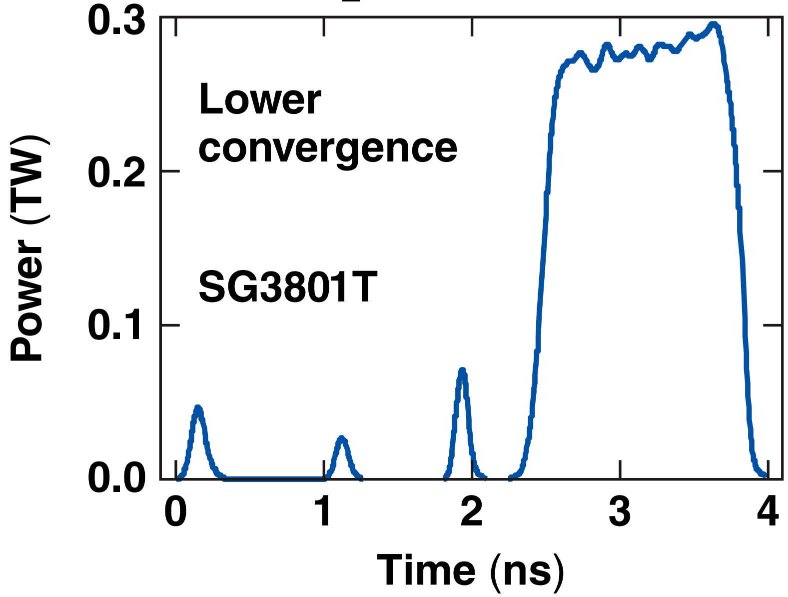

$\langle \rho R \rangle = 150$ to 200 mg/cm^2
$\langle T_i \rangle = 2.7$ to 3.0 keV

$\alpha = 2.0$
$E_L = 20$ to 25 kJ

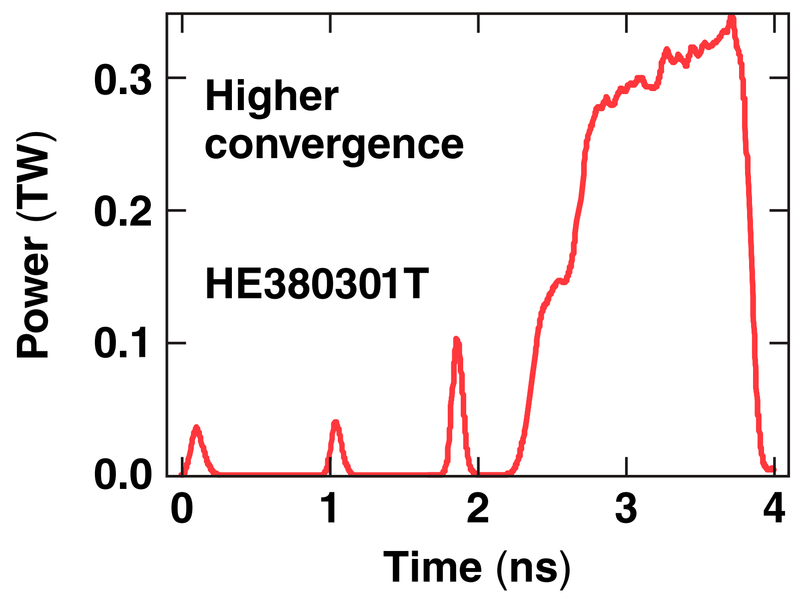

$\langle \rho R \rangle = 220$ to 320 mg/cm^2
$\langle T_i \rangle = 2.7$ to 3.0 keV

Measured areal density is determined by in-flight shell adiabat, laser coupling, and neutron sampling

- Maximum areal density in a DT implosion*

$$\rho R_{\max} = 2.6 \frac{E_{L,\mathrm{MJ}}^{1/3}}{\alpha^{0.54}}$$

- This is the absolute maximum in areal density assuming perfectly tuned implosion and
  - thin plastic overcoat (“all-DT” design)
  - laser is deposited due to inverse bremsstrahlung (no hot e^- or other LPI)
  - flux-limited thermal transport with $f = 0.06$
  - no coasting phase

*C. D. Zhou and R. Betti, Phys. Plasmas 14, 072703 (2007).

Coasting phase leads to a reduced areal density

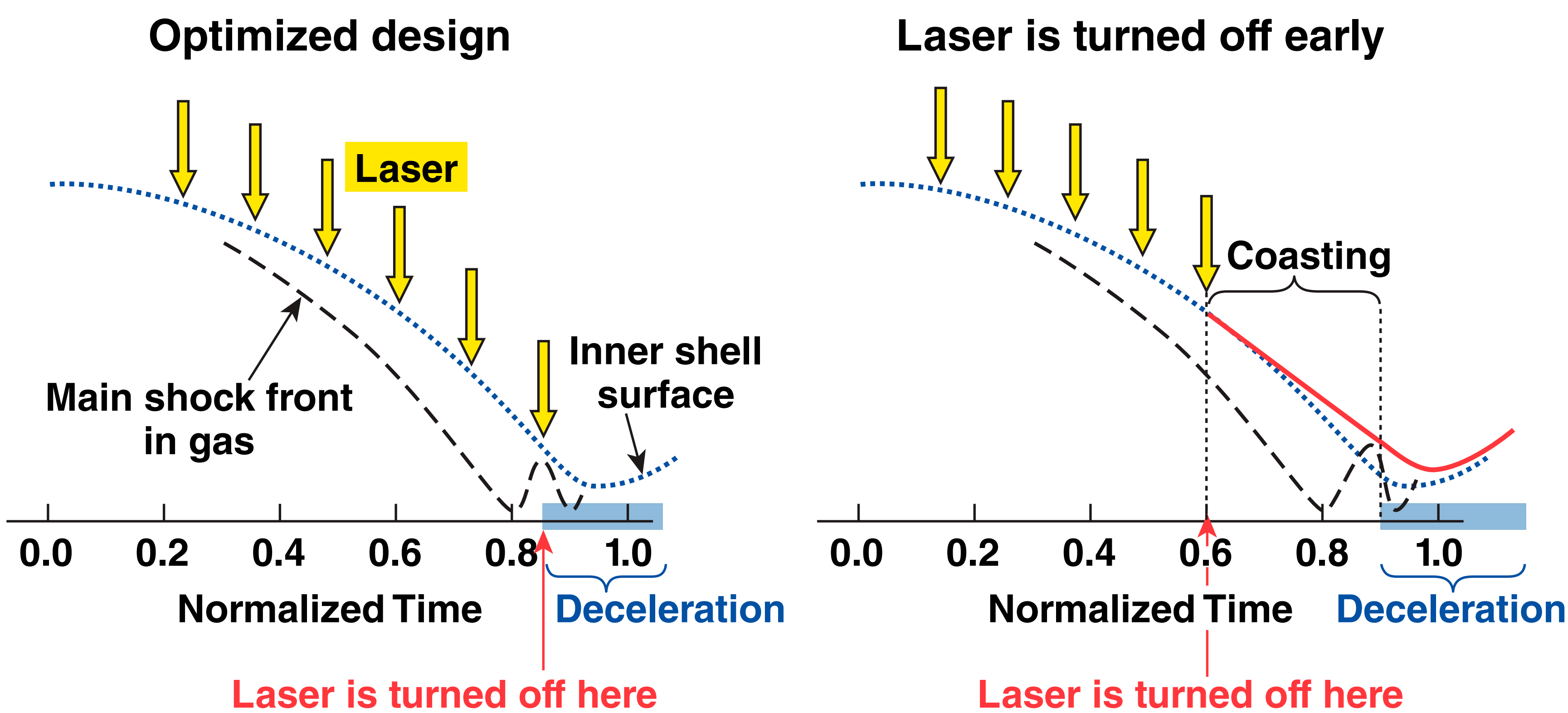

TC9271

Shell decompresses during coasting phase

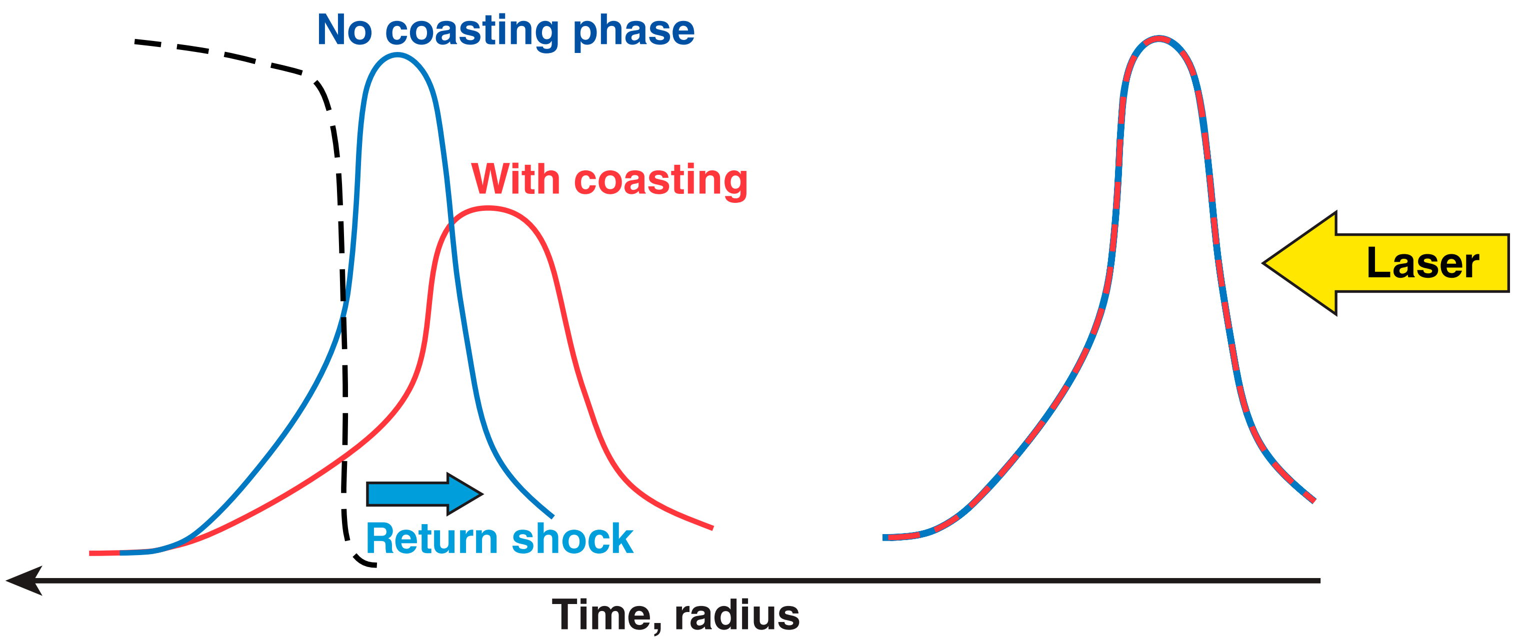

- Return shock sets the shell on higher adiabat (α_{stag}) if shell density is lower, leading to lower peak ρR
- In-flight density is reduced by coasting phase or higher in-flight α
  - in-flight adiabat is set by shocks launched at the beginning of drive
  - duration of coasting phase is determined by drive efficiency

Measured areal density is determined by in-flight shell adiabat, laser coupling, and neutron sampling

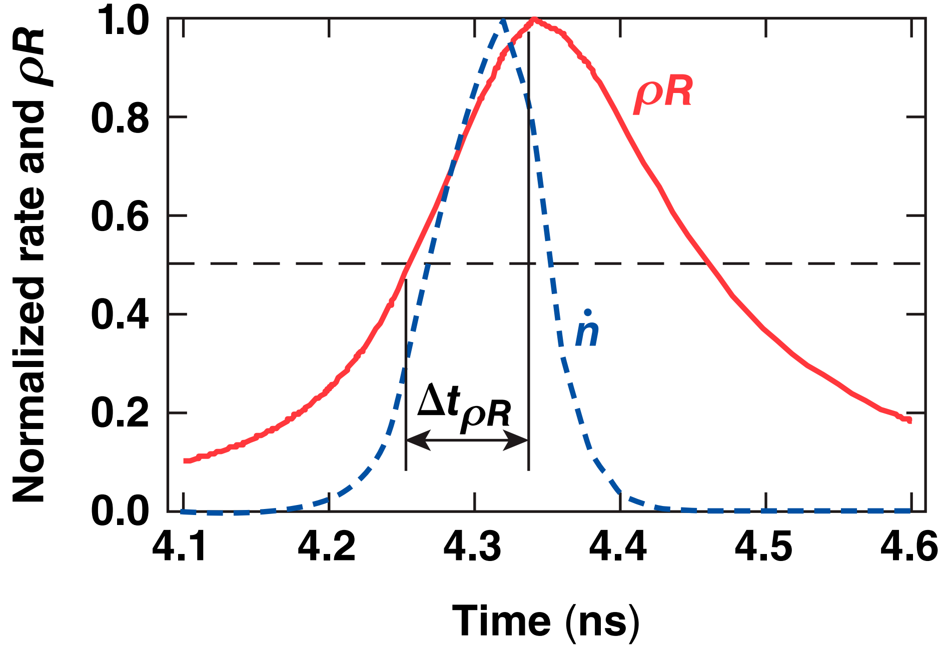

Hydro time scale during deceleration $\frac{1}{2}\Delta t_{\rho R} \approx \frac{r_{hs}}{V_{imp}} \approx \frac{20 \times 10^{-4}}{3 \times 10^{7}} = 70$ ps

$\boxed{\frac{1}{2}\Delta t_{\rho R} \approx \Delta t_n}$ ⟵ Depends on conduction losses, perturbations, e–i coupling

Timing and width of d*n*/dt relative to ρR curve depends on 3-D effects, laser coupling, adiabat, etc.

In-flight shell adiabat is tuned using VISAR shock-velocity measurements with cone targets

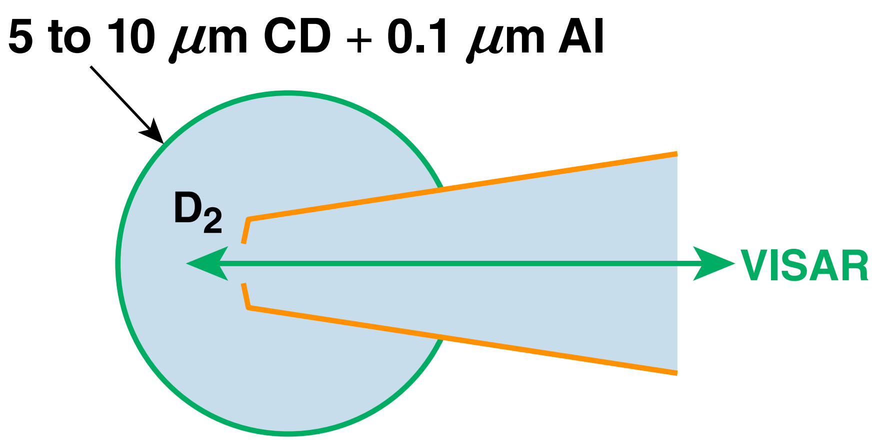

Velocity Interferometry System for Any Reflector

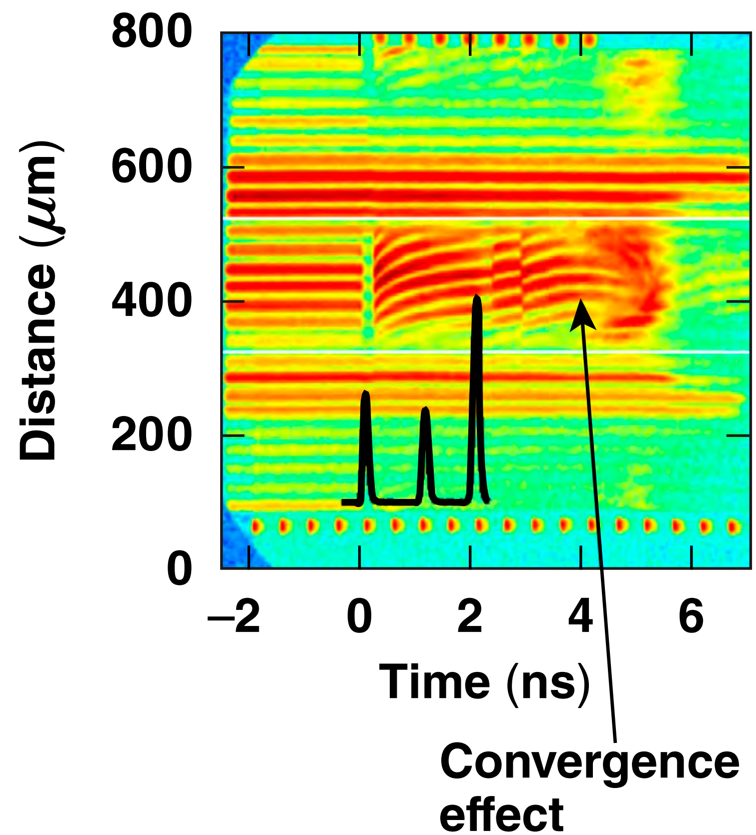

TC9014a

T.R. Boehly, accepted for publication in Phys. Rev. Lett.

The nonlocal transport model* is used to simulate shock-velocity data

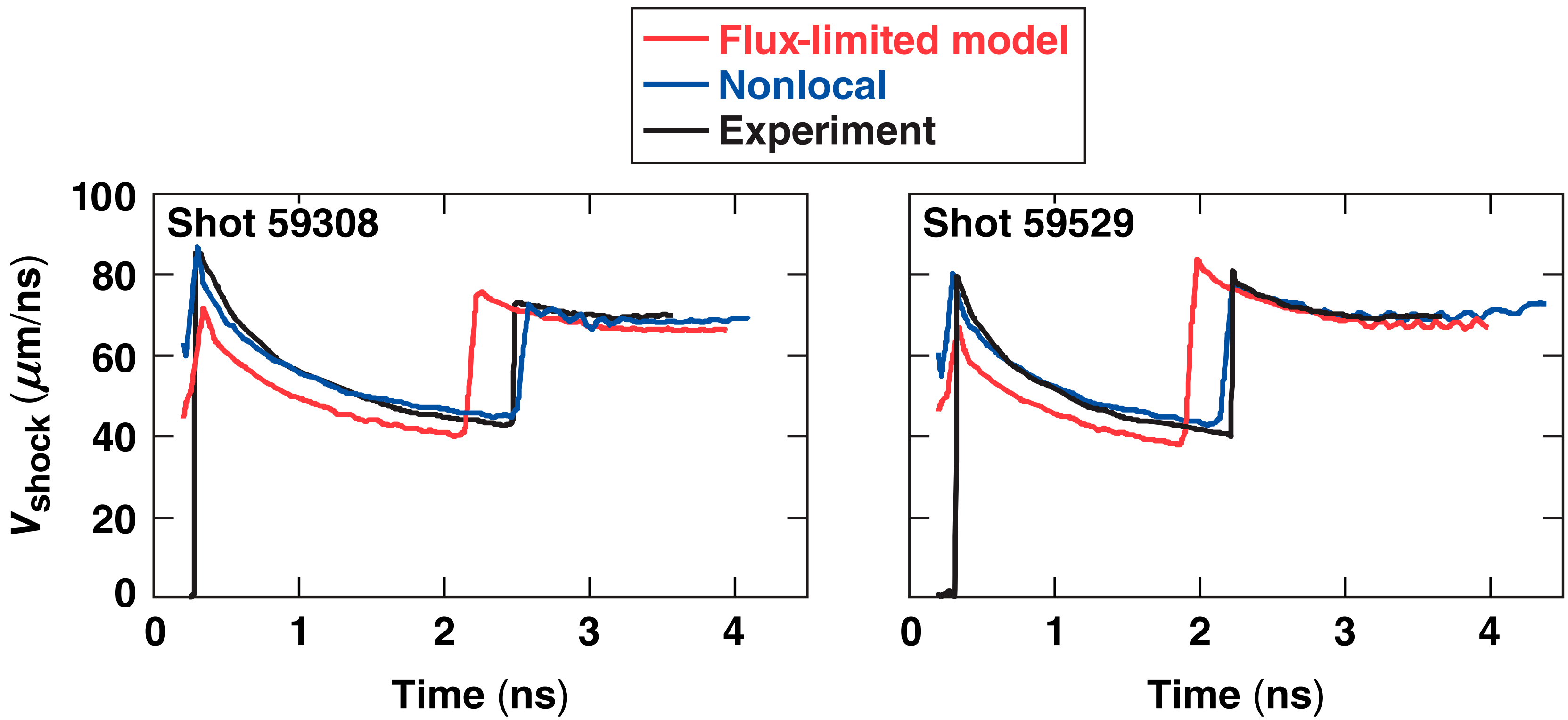

*V. N. Goncharov *et al*., Phys. Plasmas 15, 056310 (2008).

Simulations reproduce shock-velocity data very well for a variety of picket energies and picket timings

UR LLE

10-μm-thick CD shell

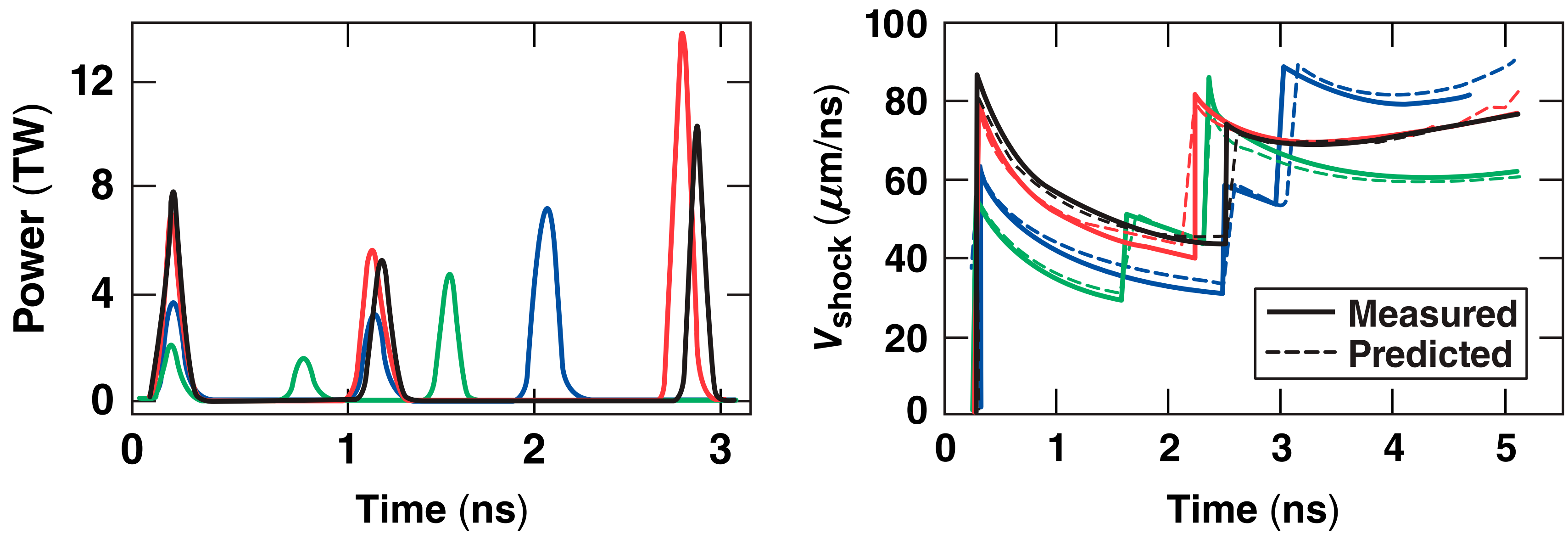

Accuracy in shock-velocity prediction meets the ignition requirement.

TC9016a

Velocities up to 135 μm/ns were measured for the shock launched by the main pulse

10-μm shell, shot 60303

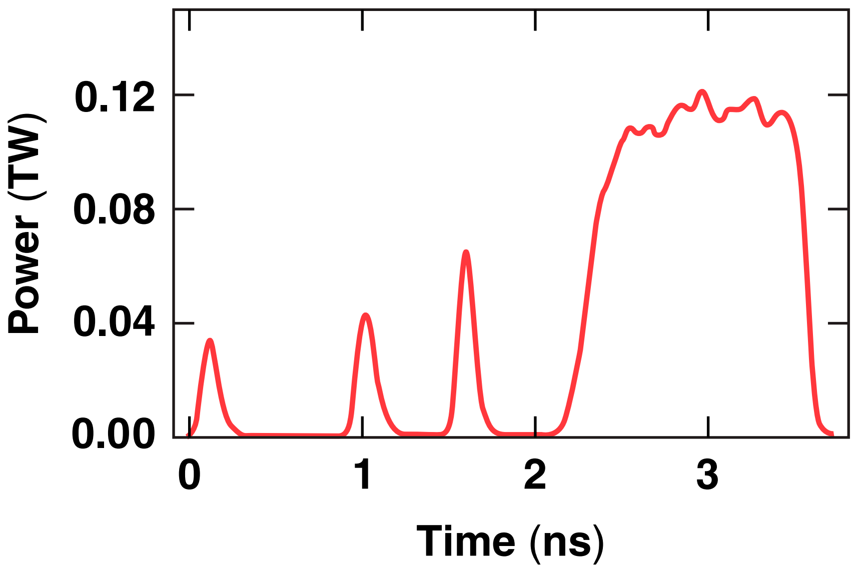

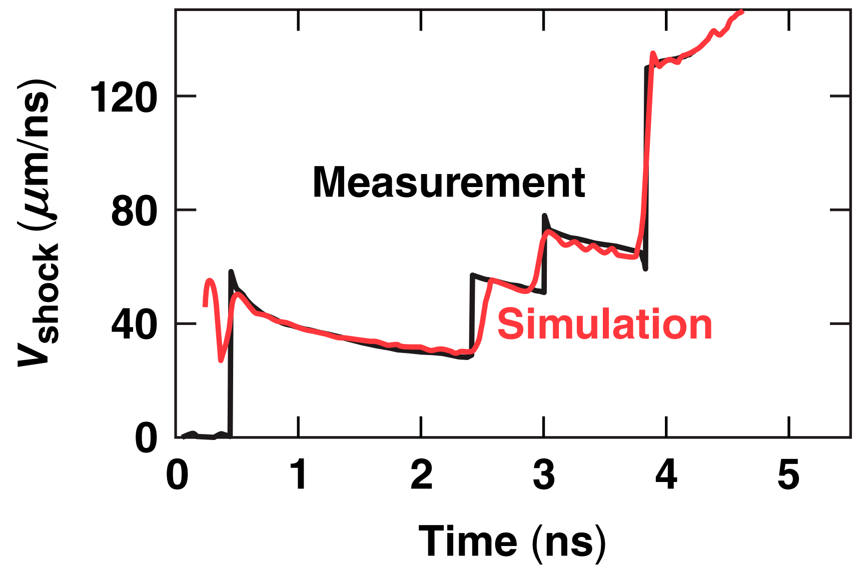

To account for shell decompression during coasting, laser coupling must be accurately modeled

Diagnostics to verify hydrodynamic efficiency ($E_{k,\,\mathrm{shell}}/E_{\mathrm{laser}}$)

- NTD timing
  - PROs
    - sensitive to small variations in implosion velocity
  - CONs
    - time-integrated effect, not a unique shell-velocity solution
- Scattered-light measurement
  - PROs
    - time-resolved measurement
  - CONs
    - not all absorbed light contributes to the drive—
      not a direct measurement of hydro-efficiency

Areal Density

The measured bang time is later than predictions for both designs

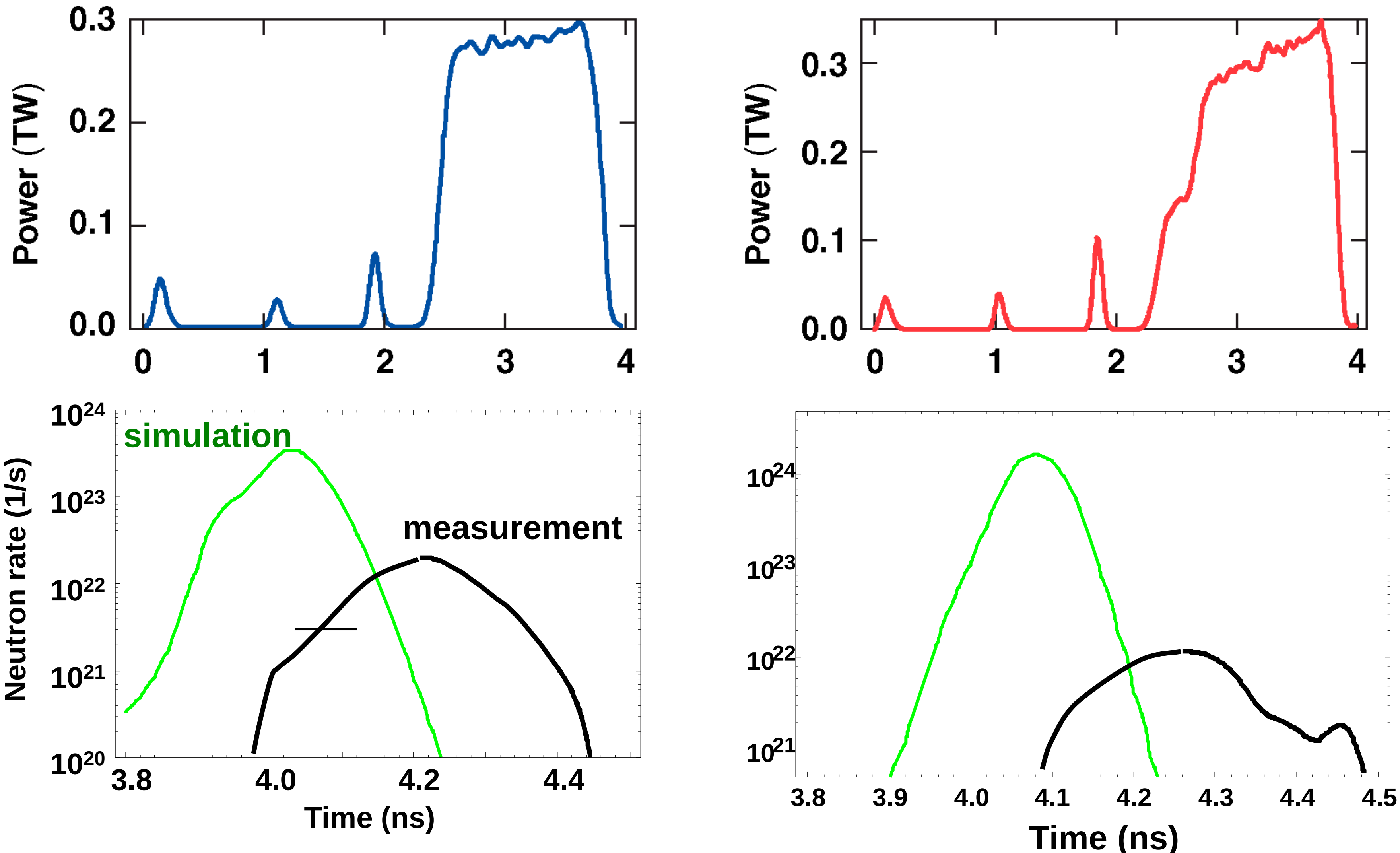

Scattered light measurements show a reduced laser energy absorption

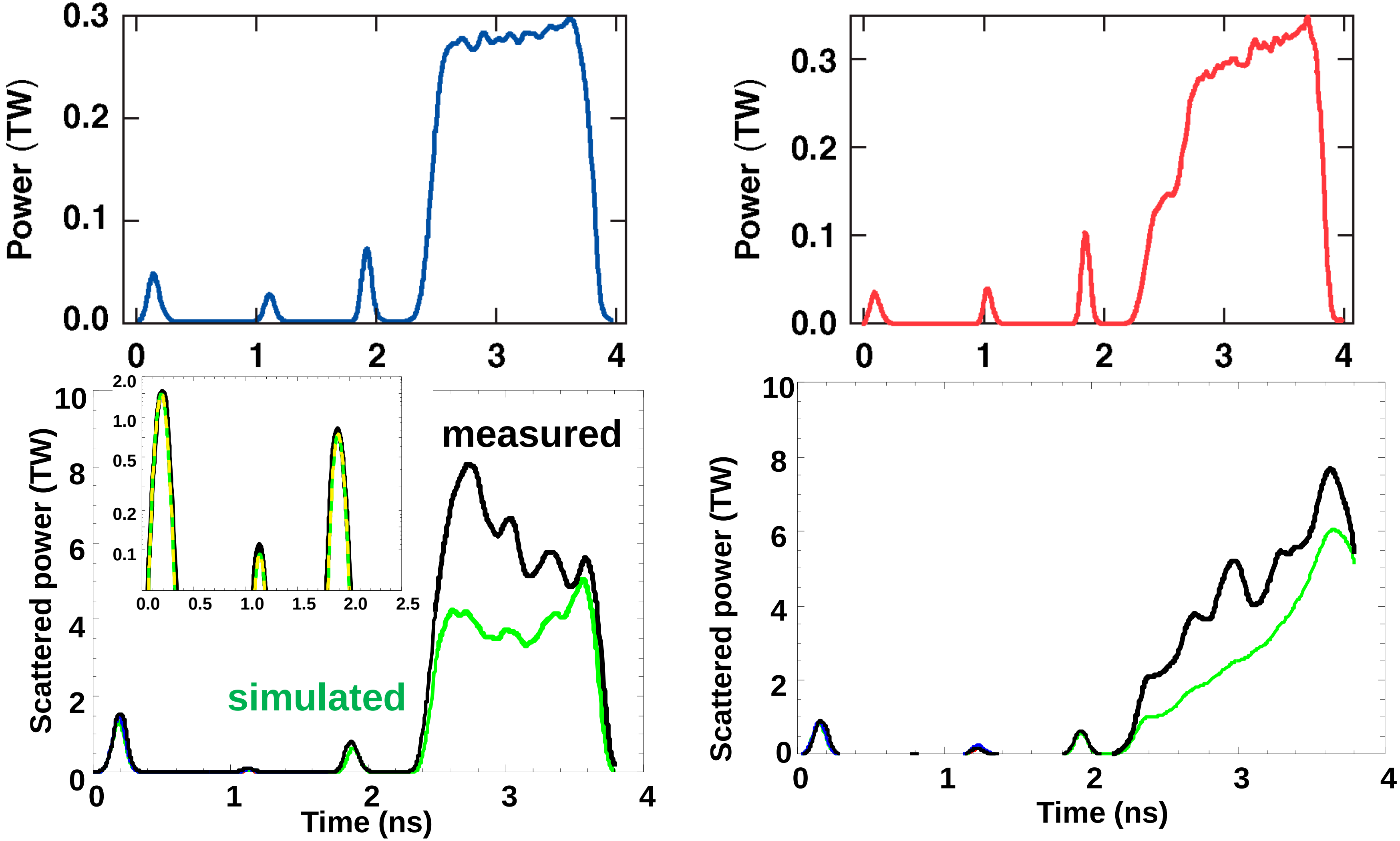

Beam-to-beam energy transfer leads to a reduction in laser coupling[1]

The transfer of energy from (1) to (2) is due to SBS before deposition[2]

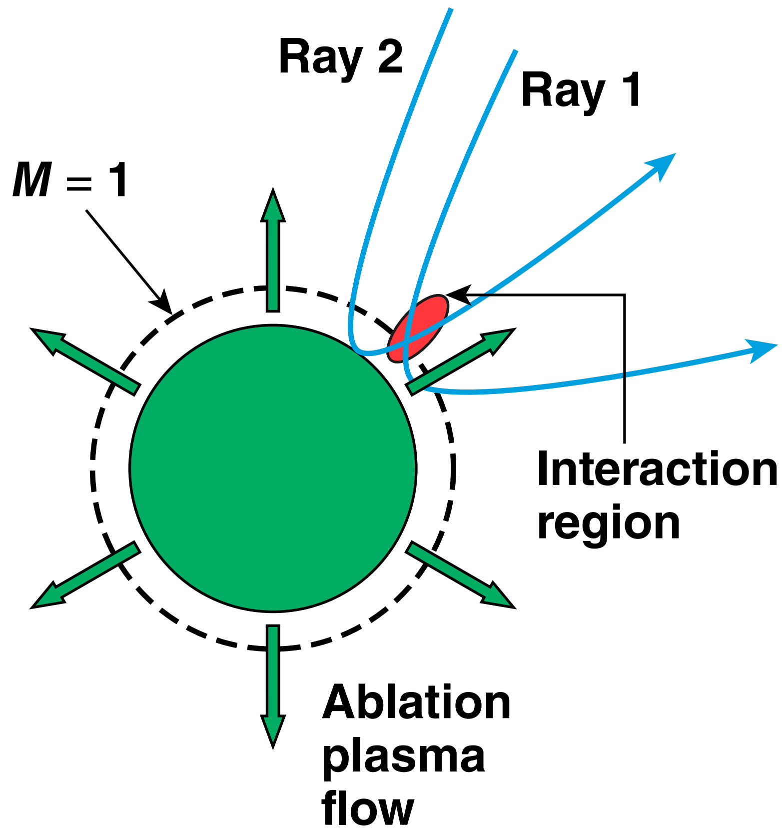

[1] I. V. Igumenshchev *et al*., "Cross-Beam Energy Transfer in ICF Implosions on OMEGA," submitted to Phys. Plasmas.
[2] C. J. Randall, J. R. Albritton, and J. J. Thomson, Phys. Fluids 24, 1474 (1981).

TC8901b

Combination of cross-beam transfer and nonlocal model reproduce bang time measurements

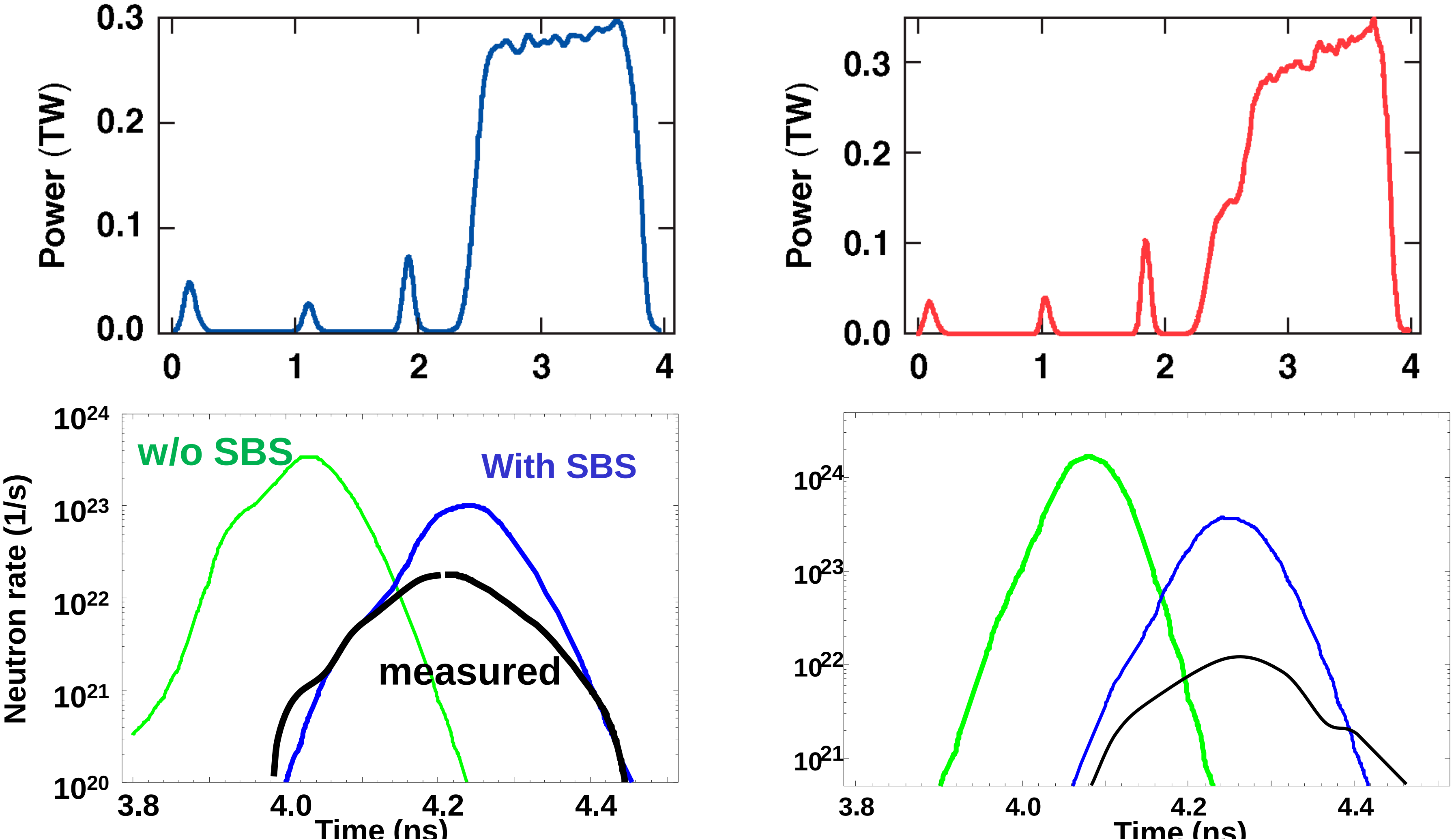

Combination of cross-beam transfer and nonlocal model reproduce scattered light measurements

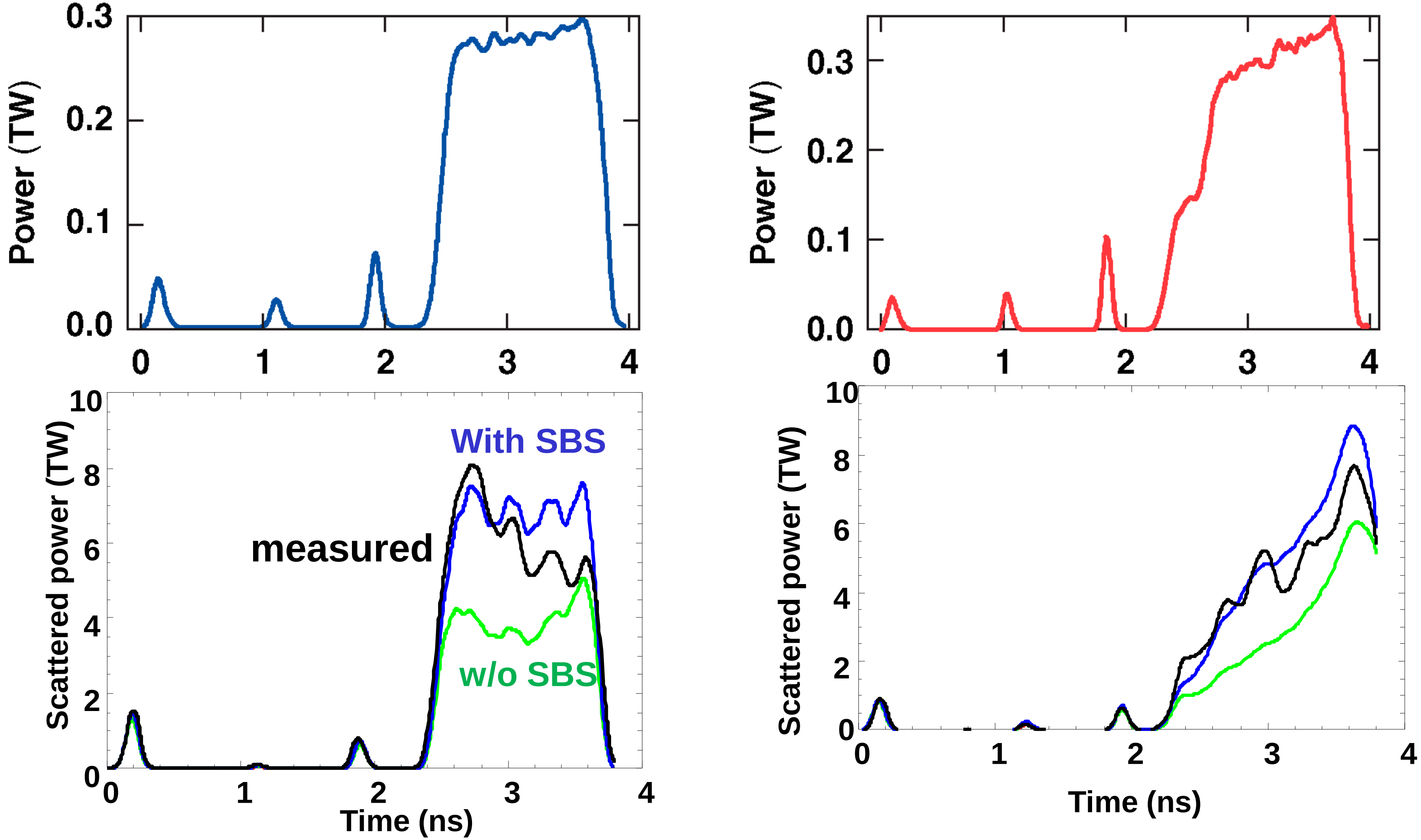

Deviations in scattered-light data from predictions at late time correlate with excitation of TPD instability

UR LLE

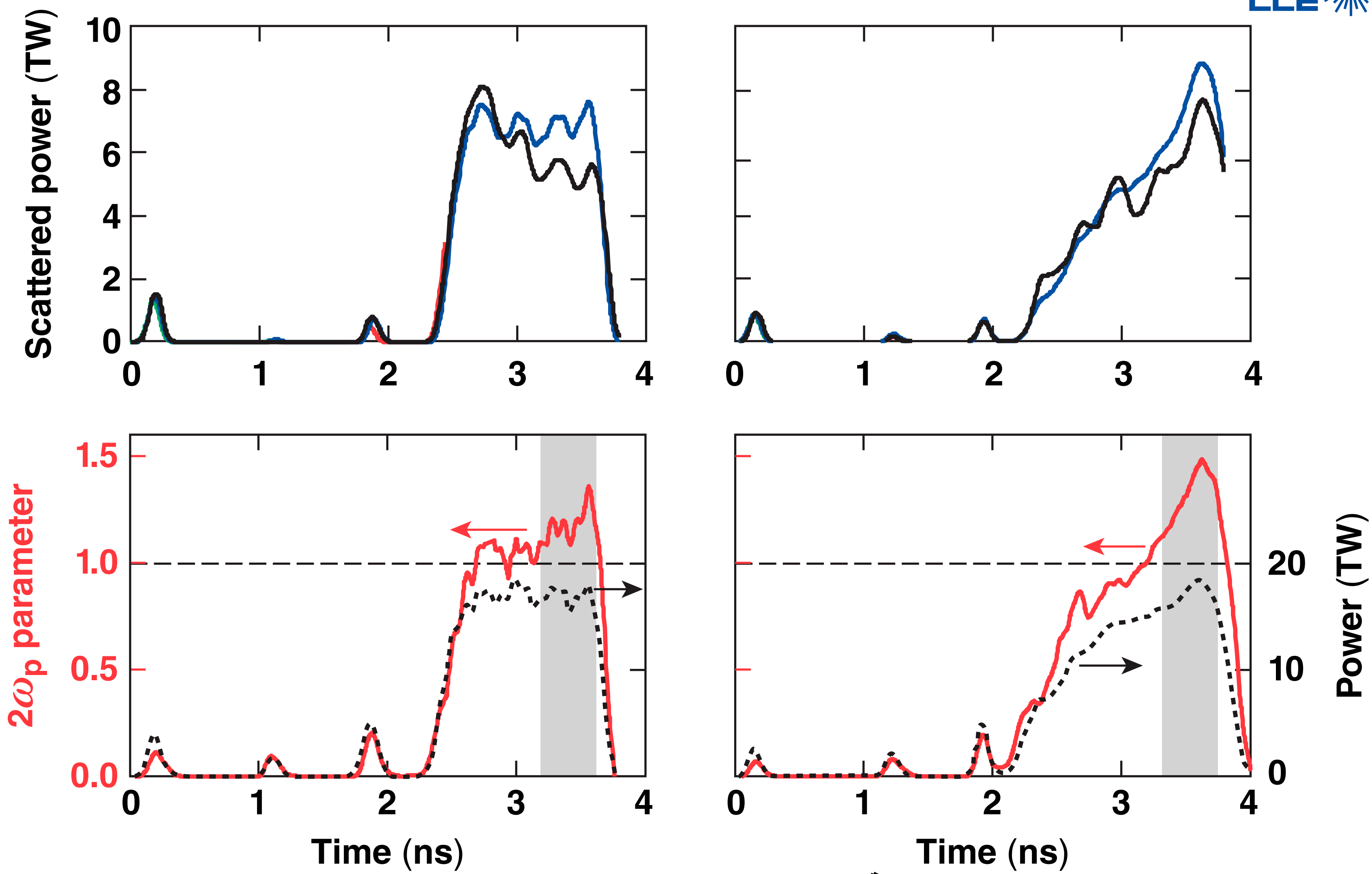

$2\hat{\omega}_p$ parameter $= I_{14}\,L_n(\mu m)/230\,T_{keV}$

TC9283

Deviations start earlier when drive intensity is higher

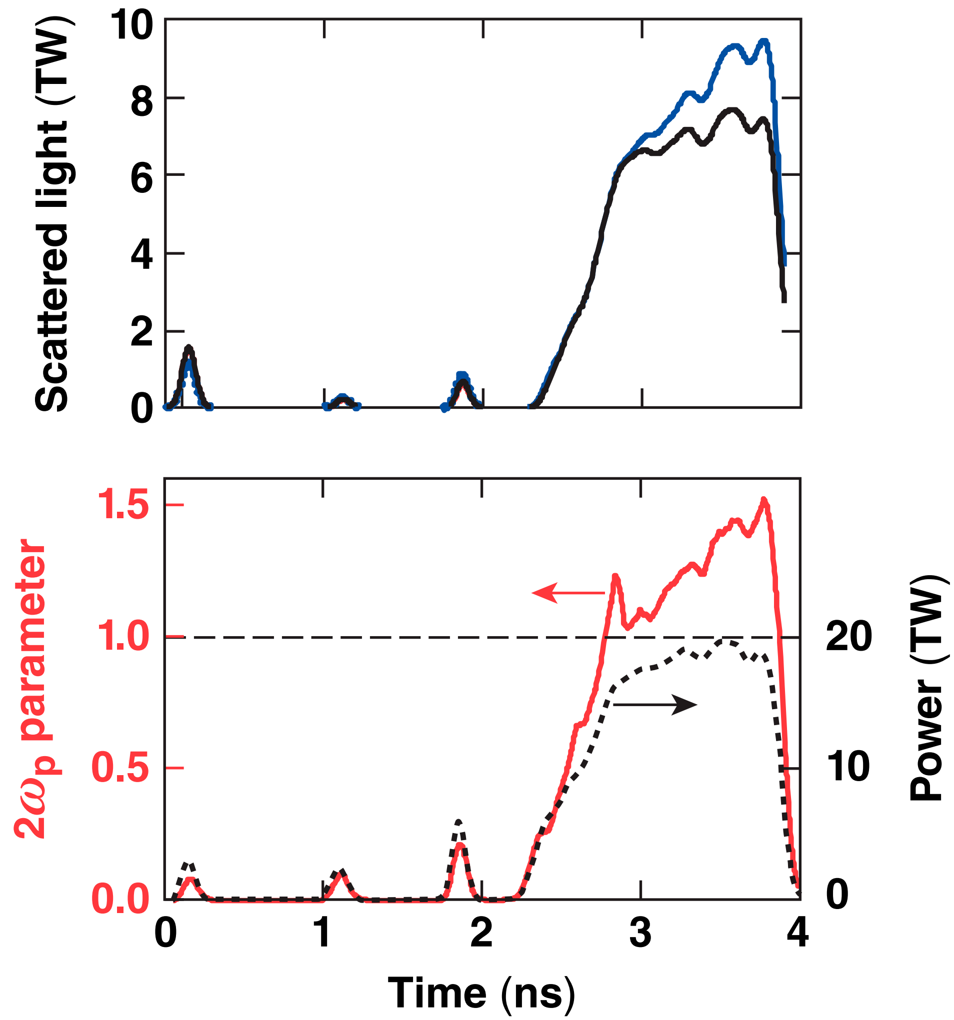

Areal density in a cryogenic-DT implosion is measured using a magnetic recoil spectrometer

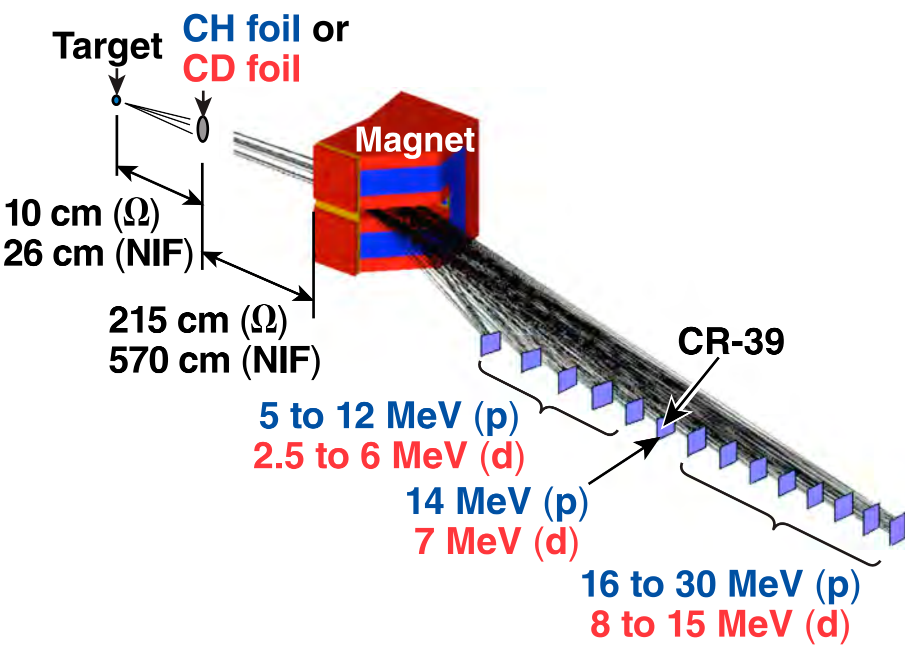

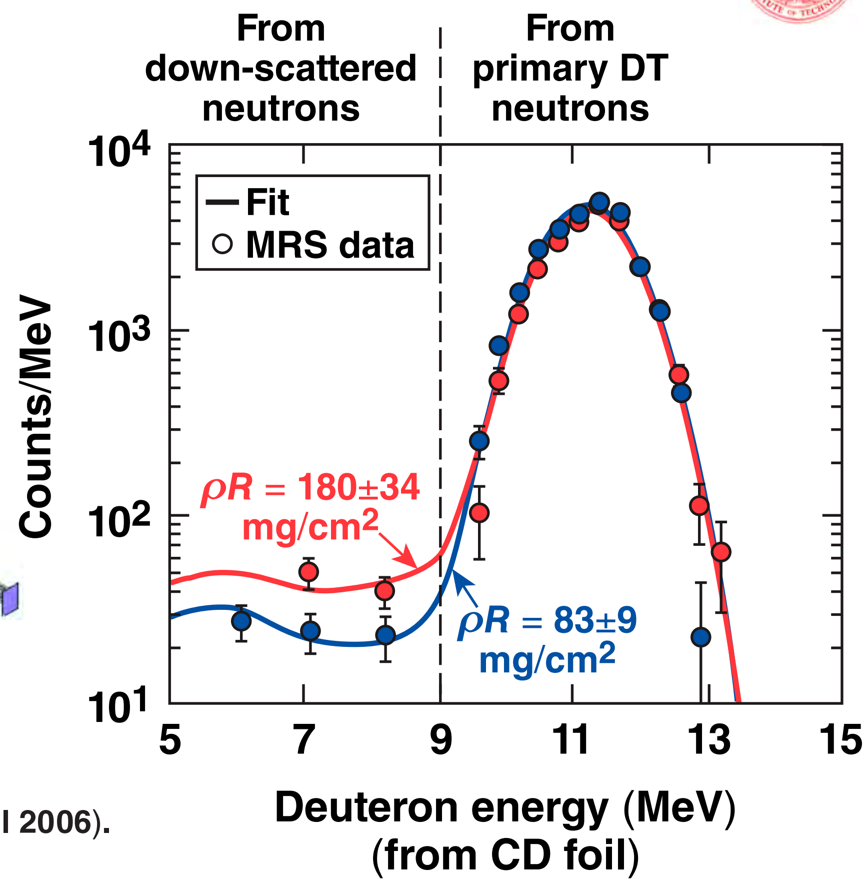

J. A. Frenje *et al*., NIF MRS System Design Review (April 2006).
J. A. Frenje *et al*., Rev. Sci. Instrum. 79, 10E502 (2008).

Areal density in a single-view MRS measurement is averaged over solid angle $\Omega \approx 3/2\pi$

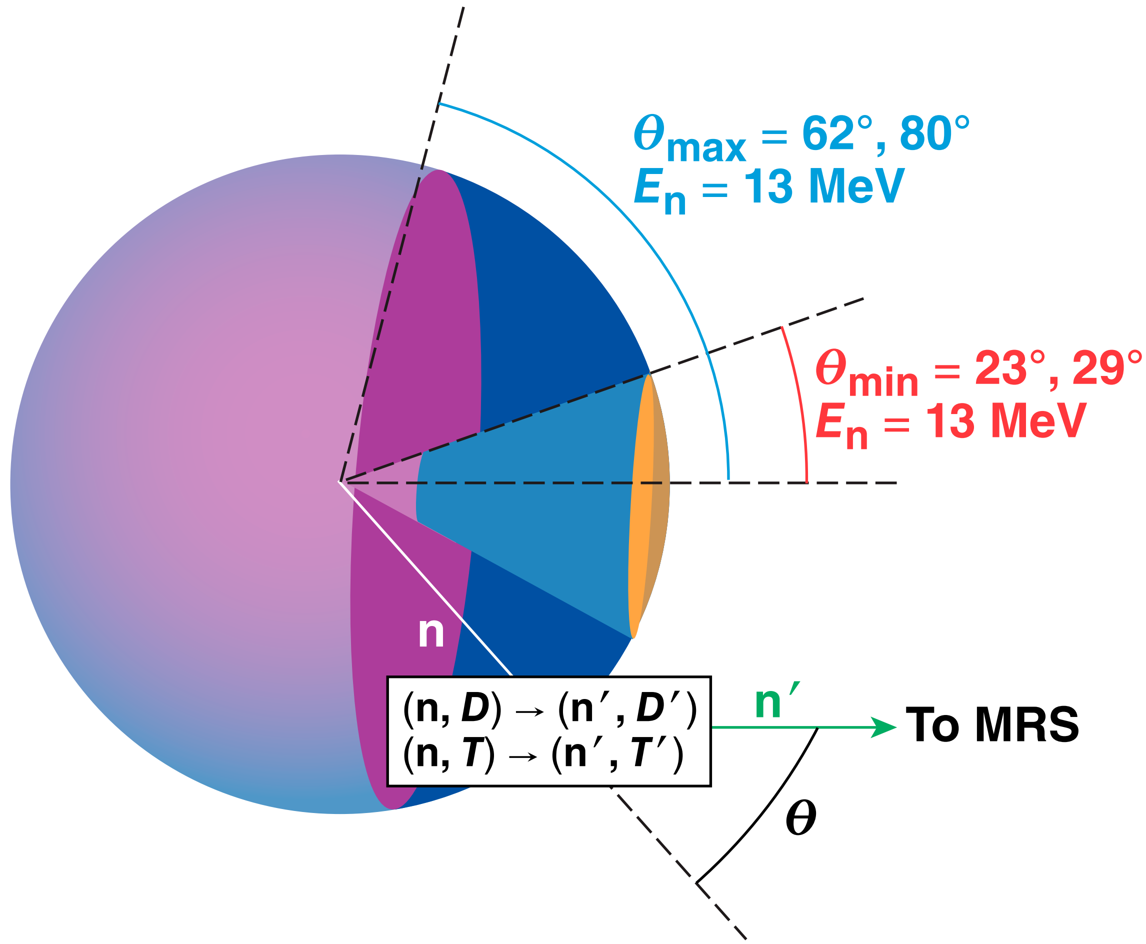

Offset > 10 μm or ice roughness with $\sigma_{\ell \leq 2}$ > 1 μm makes ρR measurement direction-dependent

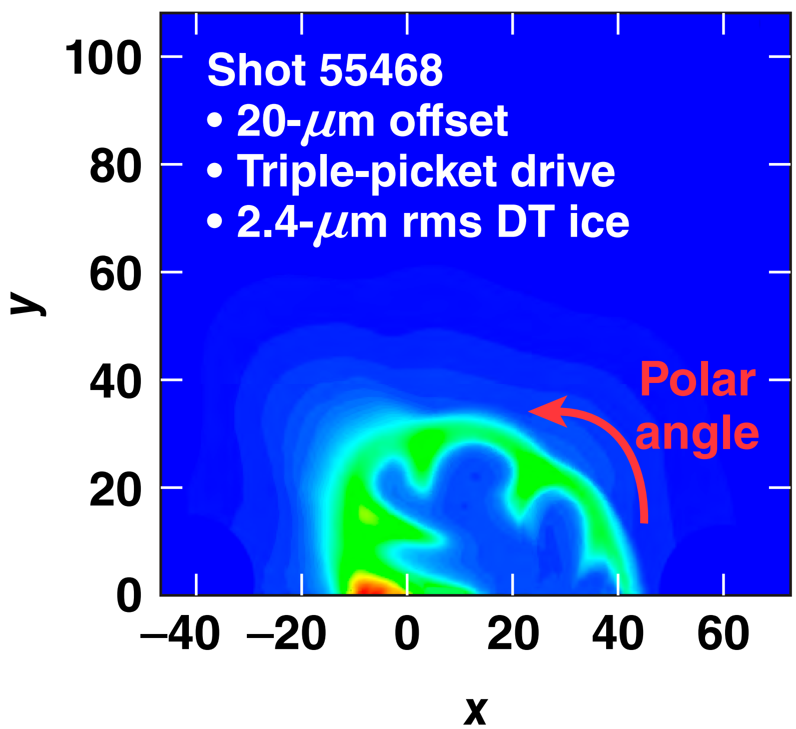

Neutron spectrum fit including MRS response and error bar

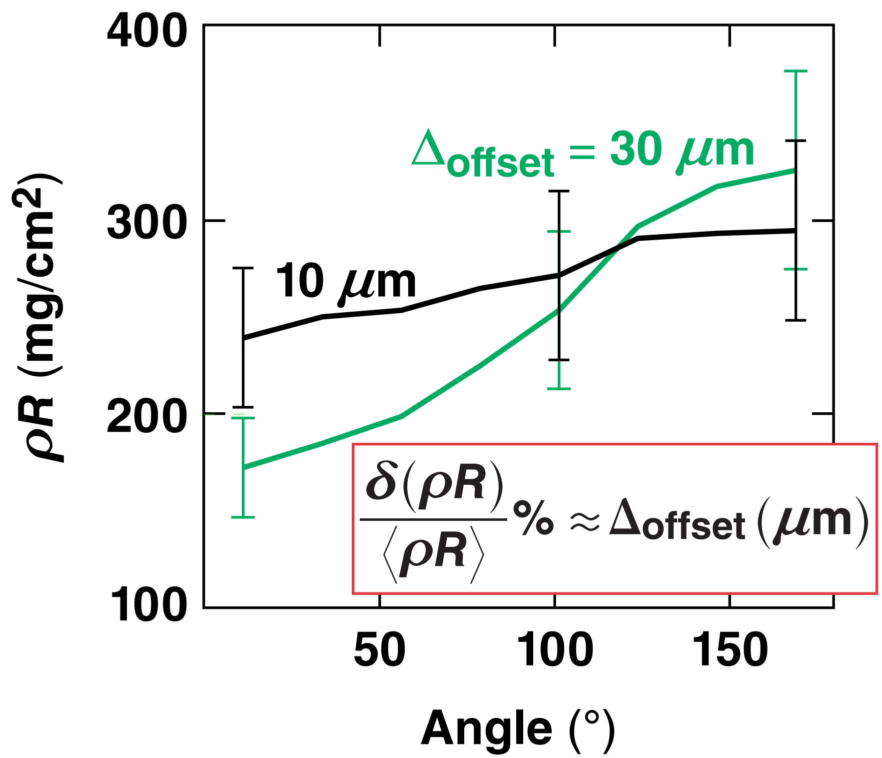

- $\delta\langle\rho R\rangle$ for 10-μm offset $\approx \delta\langle\rho R\rangle$ for ice roughness $\sigma_{\ell \leq 2}$ > 1 μm

The measured areal density in triple-picket cryogenic implosions agrees with predictions

UR LLE

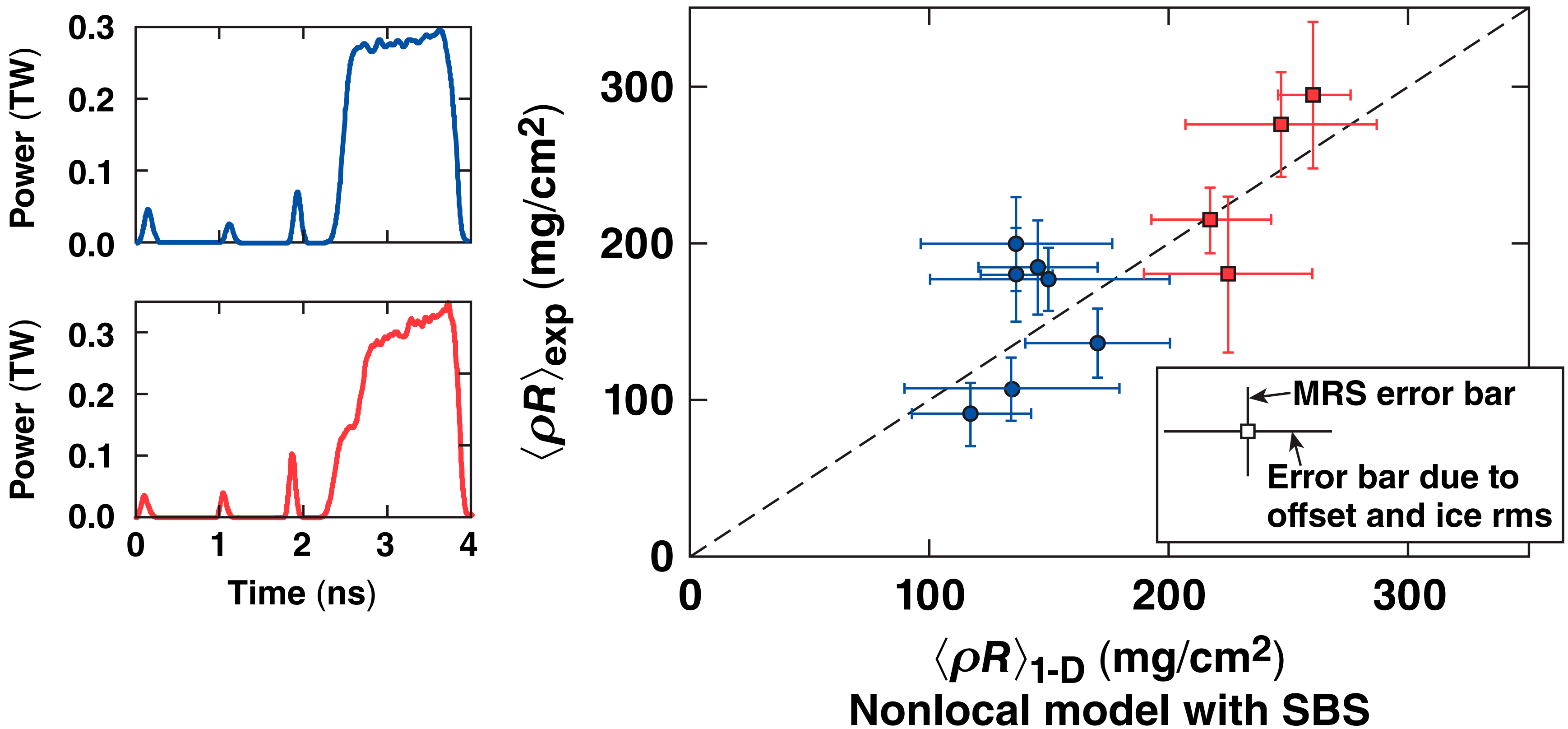

The areal-density measurements confirm accuracy of shock tuning and shell stability to short-wavelength perturbations.

TC9290

5-µm-thick CD shells are considered to take advantage of higher hydrodynamic efficiency of DT ablator

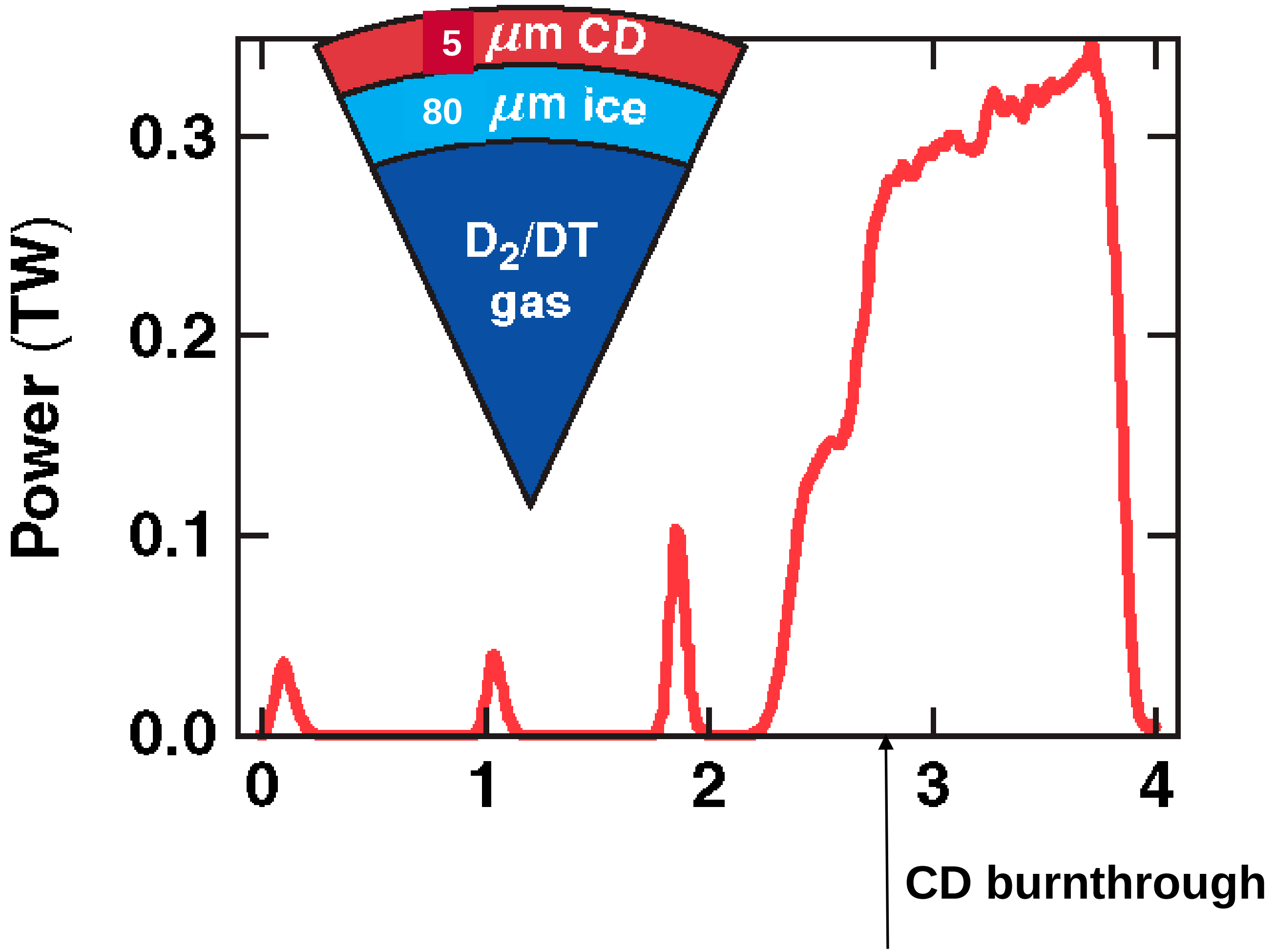

- Thermal conduction ~1/Z ⟹ DT is more efficient ablator

Predicted and measured scattered light power disagree after CD burns through

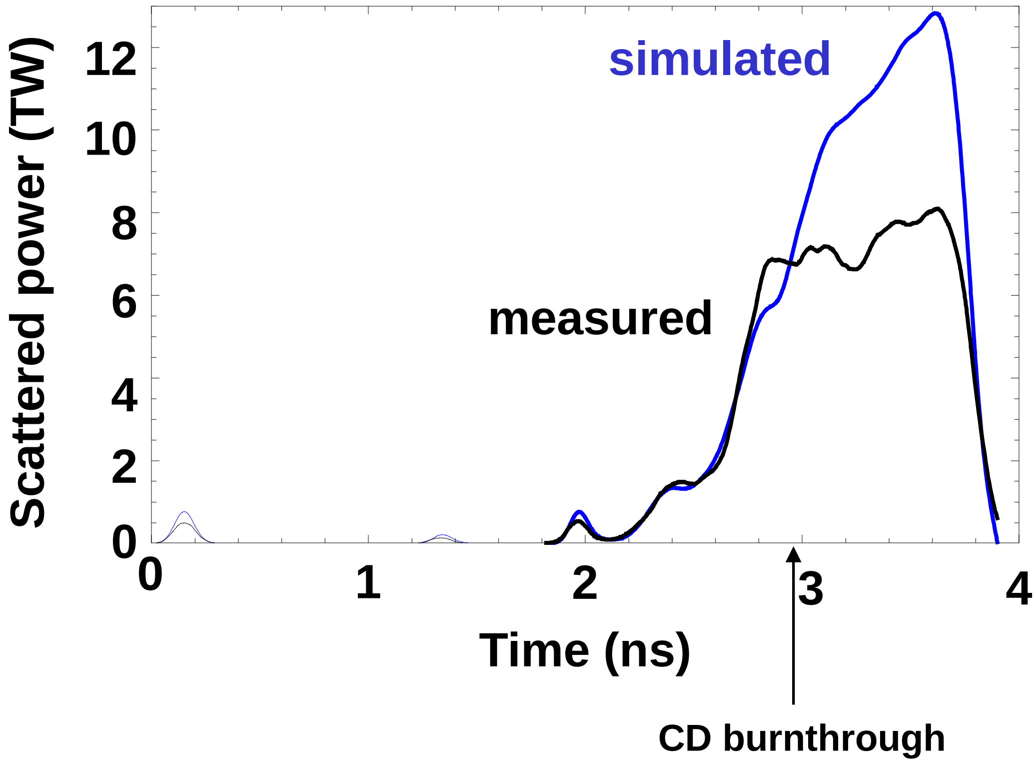

$2\omega_p$ parameter is larger for DT ablator because of lower T_e and higher intensity at $n=n_c/4$

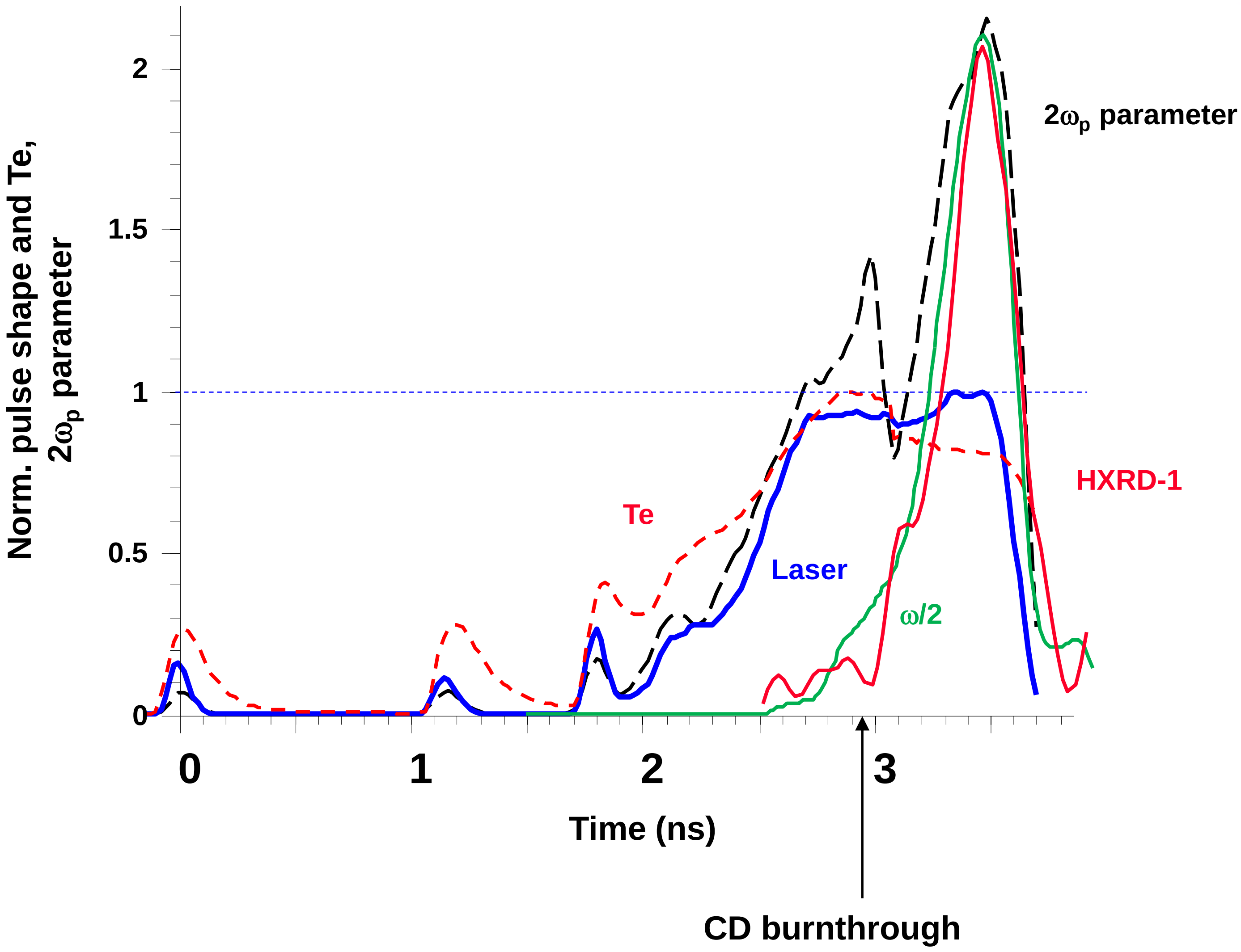

Simulations predict higher perturbation growth at CD-DT interface for thin-CD ablators*

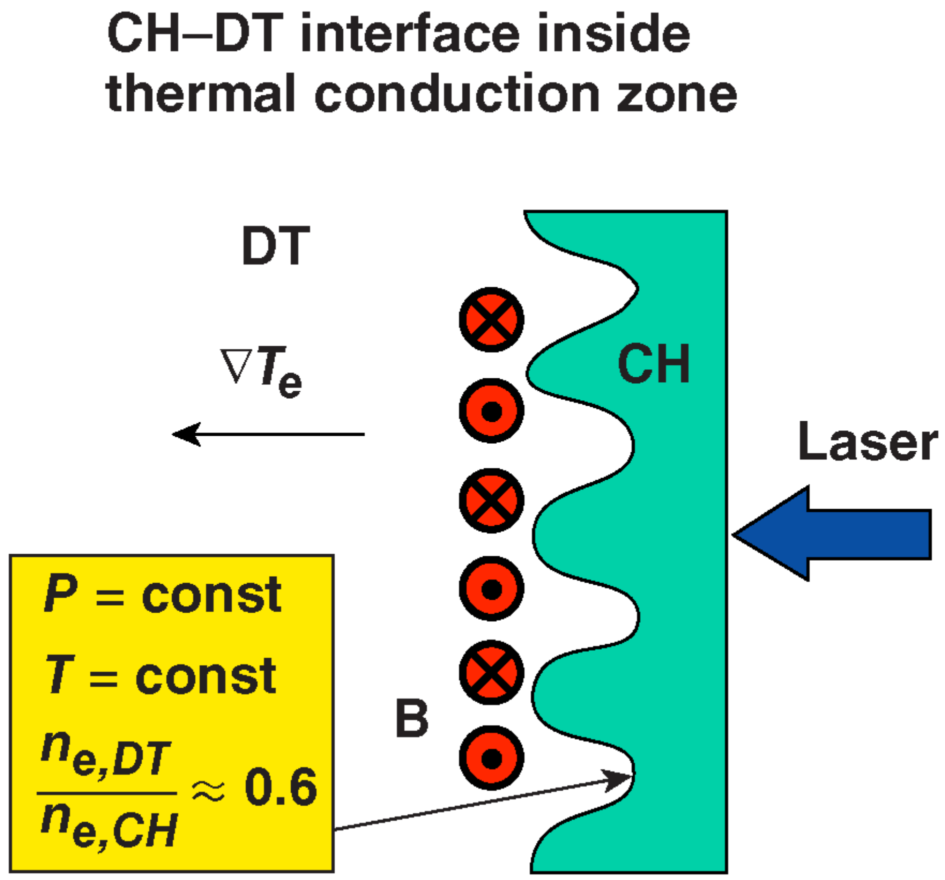

* I. Igumenshchev, APS 2010

Simulations predict higher perturbation growth at CD-DT interface for thin-CD ablators

Cryogenic target in the middle of the main pulse: magnetic fields at CH ablation surface*

t = 3.2 ns

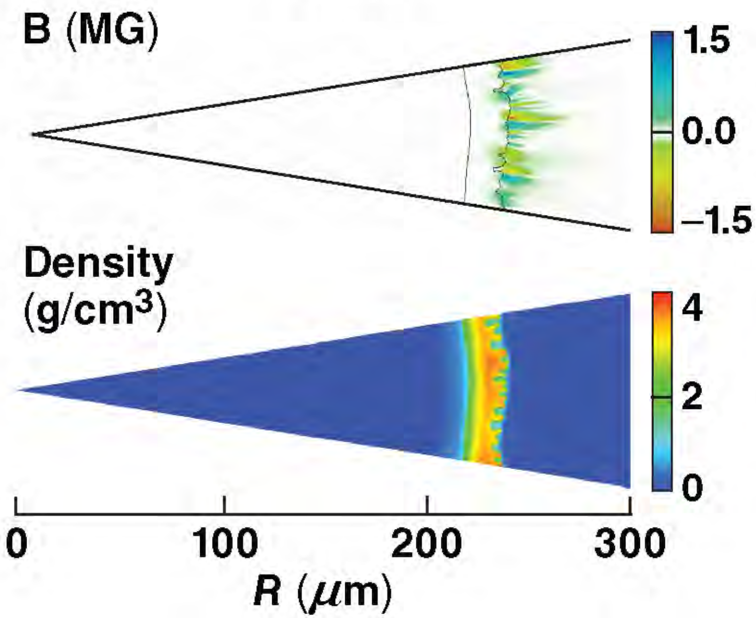

CH is all ablated: magnetic fields at CH–D interface

t = 3.5 ns

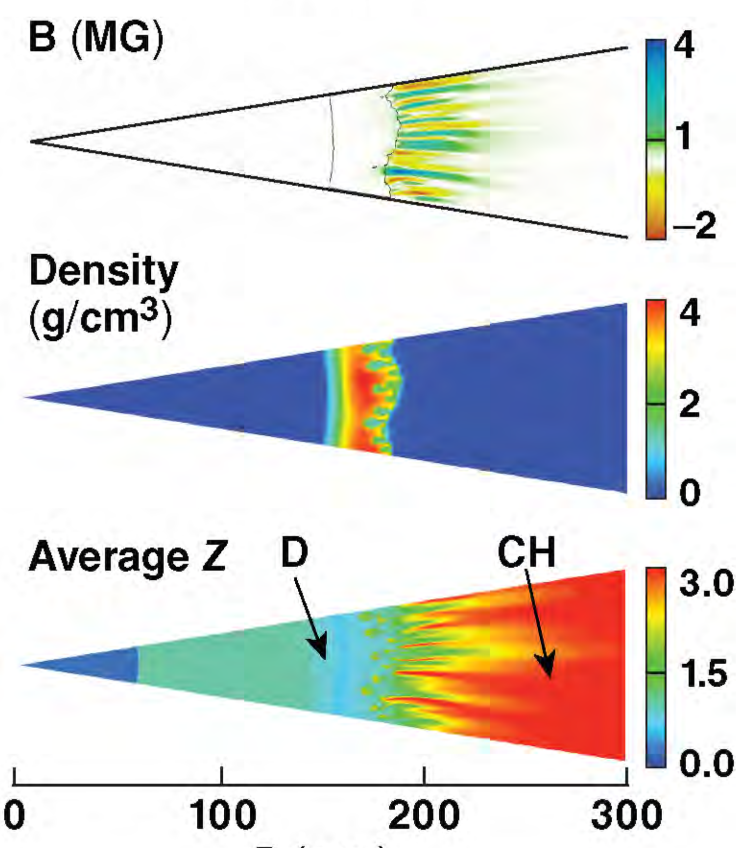

Summary/Conclusions

Modeling of cryogenic implosions on OMEGA is approaching precision required for ignition

- The majority of the observables are consistent with calculations when the nonlocal thermal transport is used and the effect of cross-beam energy transfer is taken into account in the laser-deposition modeling
- Areal densities measured in cryogenic implosions are in agreement with 1-D predictions
- At current levels of nonuniformity sources (offset, ice roughness, condensables, ablator finish), measured ion temperature is lower than 1-D calculation by ~20% and yield is ~5% to 10% of 1-D predictions
- With improved nonuniformity, cryogenic implosions on OMEGA are predicted to achieve YOC ~15% to 20% with $\langle T_i \rangle$ ~90%$\langle T_i \rangle_{1\text{-D}}$

With the best smoothing, the measured ion temperature is ~20% lower than the predicted value

Cryogenic Implosions

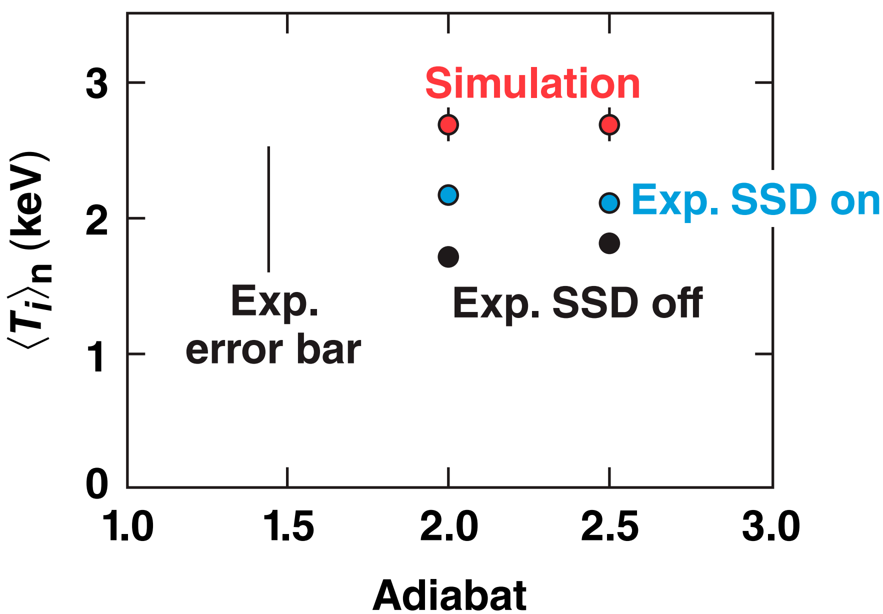

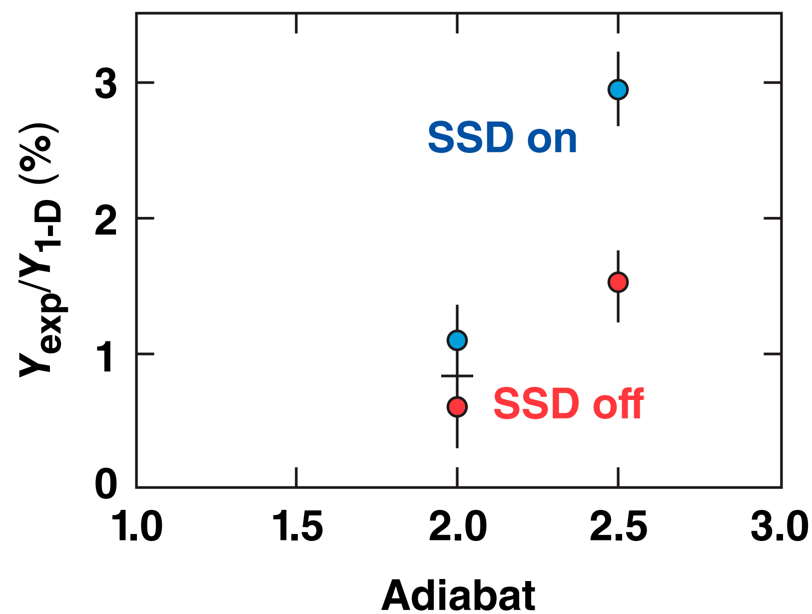

TC9291

Ion temperature is inferred from the temporal width of neutron time of flight (nTOF)

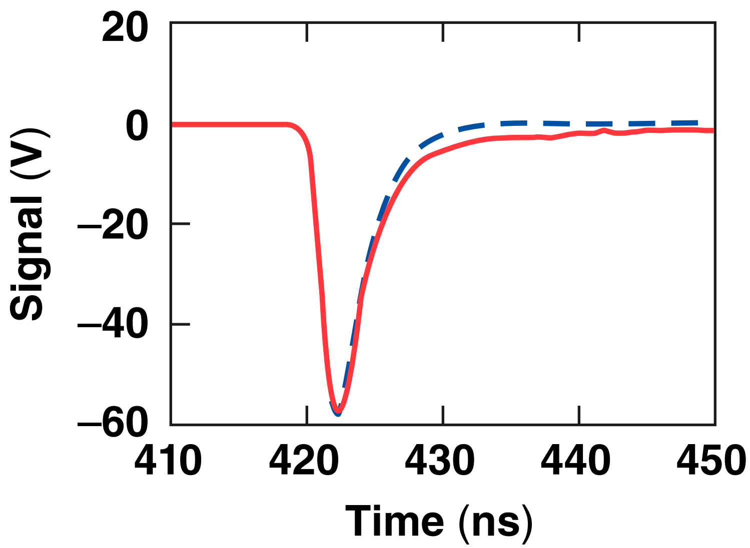

Signal	Rise	Fall
–106.01	0.81	2.20

$$\Delta t\,(\text{ps}) = 122\,d\,(m)\sqrt{T_i\,(\text{keV})}$$

$d = 5$ m

$T_i = 2$ keV

$\Delta t = 900$ ps

Only two parameters: fall slope and detector response for each nTOF

$$m(t) = \frac{A}{2\tau}\exp\left[-\frac{(t-t_1)}{\tau}\right]\times\exp\left(\frac{\sigma^2}{2}\right)\left\{1+\mathrm{erf}\left[\frac{(t-t_1)-\sigma^2/\tau}{\sqrt{2\sigma^2}}\right]\right\}^{*}$$

*T. J. Murphy *et al.*, Rev. Sci. Instrum 86, 610 (1997).

Neutron spectrum broadening is caused by thermal ion motion and bulk fluid motion

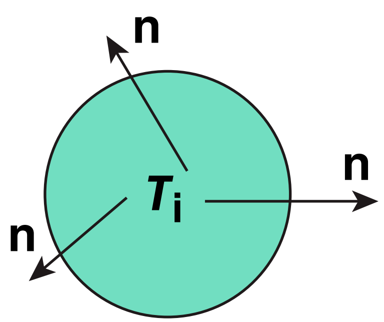

Fluid at rest

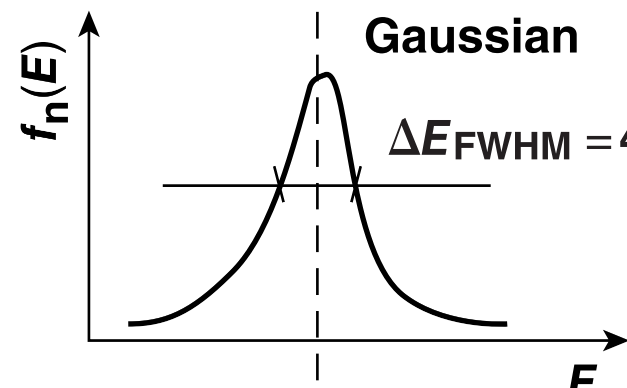

$$\Delta E_{FWHM} = 4\sqrt{\frac{M_n \log(2)}{M_n + M_a} T_i E_0} = 177\sqrt{T_i\,(\text{keV})}$$

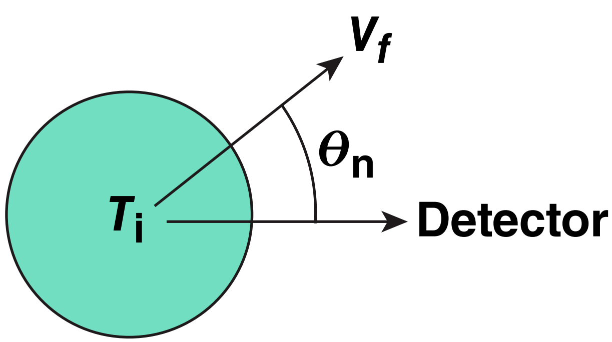

Moving fluid

$$f(E) = \exp\left[-\left(\frac{E - E_0}{\Delta E} - M_a \cos\theta_n\right)^2\right]$$

$$M_a = \frac{V_f}{c_s},\ c_s = \sqrt{\frac{T_i}{m_i}}$$

Flow with spherical symmetry leads to spectral broadening

$$f(E) = \exp\left[-\left(\frac{E-E_0}{\Delta E} - M_a \cos\theta_n\right)^2\right]$$

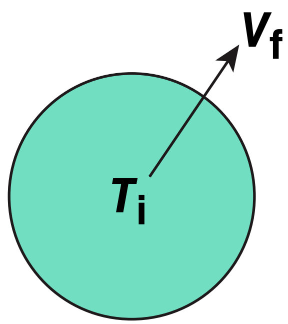

Whole plasma moves in one direction

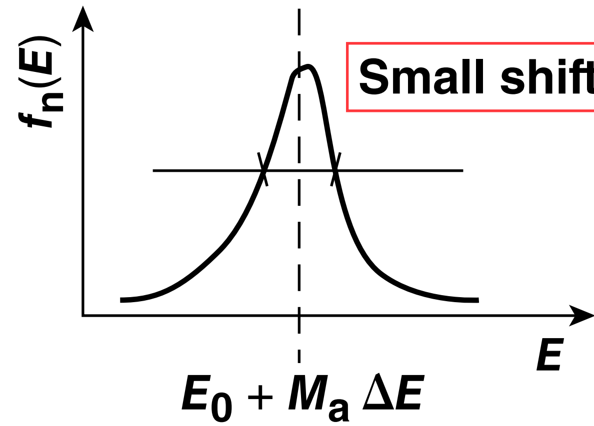

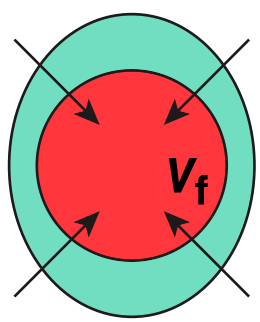

Radial motion

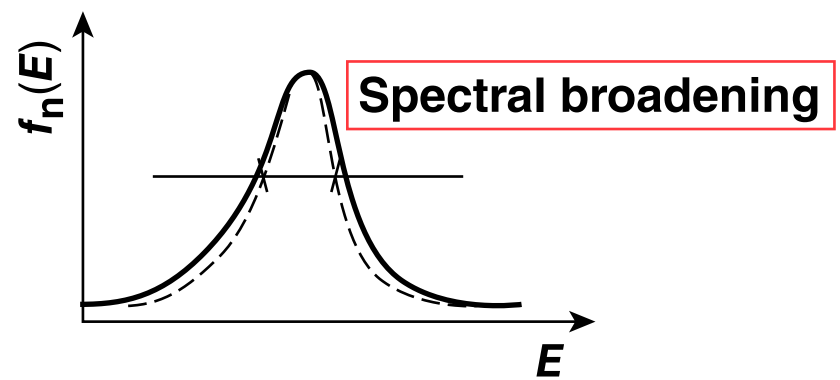

$$f(E) = \frac{\sqrt{\pi}}{2\,M_a}\left[\mathrm{erf}\left(\frac{E-E_0}{\Delta E} + M_a\right) - \mathrm{erf}\left(\frac{E-E_0}{\Delta E} - M_a\right)\right]$$

T_i calculated from reaction-averaged neutron energy width must be compared with $\langle T_i \rangle_n$

$$\langle T_i \rangle_n = \frac{\int dt \int dV n^2 \langle \sigma v \rangle T_i}{\int dt \int dV n^2 \langle \sigma v \rangle}$$

$$\langle f \rangle = \frac{\int dt \int dV n^2 \langle \sigma v \rangle f}{\int dt \int dV n^2 \langle \sigma v \rangle} \propto \exp\left[-4 \log(2) \left(\frac{E - E_0}{\Delta E_{fit}}\right)^2\right]$$

$$\langle T_i \rangle_{fit} (\mathrm{keV}) = \left(\frac{\Delta E_{fit}\,(\mathrm{keV})}{177}\right)^2$$

For a spherically symmetric implosion

$$\langle T_i \rangle_{fit} (V_{flow} = 0) < \langle T_i \rangle_n$$

$$\langle T_i \rangle_{fit} (V_{flow} \neq 0) \approx \langle T_i \rangle_n$$

Temperature gradient inside the hot spot leads to a reduction in $\langle T \rangle_{fit}$ with respect to $\langle T \rangle_n$

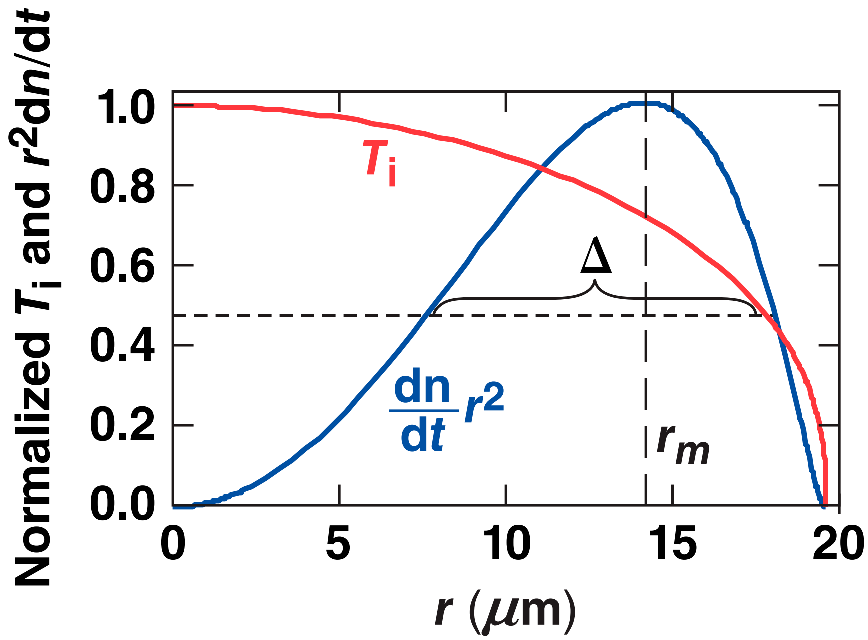

$$T_i \approx T_0 \left(1 + \frac{r - r_0}{L_T}\right) + T_0'' \frac{(r - r_0)^2}{2}$$

$$\langle T_i \rangle_n \sim T_0 \left(1 - \frac{1}{24} T_0'' \Delta^2\right)$$

$$\langle f \rangle \sim \exp\left[-\left(\frac{E - E_0}{\Delta E_{fit}}\right)^2\right] \Rightarrow \langle T_i \rangle_{fit} = \langle T_i \rangle_n - 0.2\, T_0 \left(\frac{\Delta}{2 L_T}\right)^2$$

Radial flow leads to an increase in $\langle T \rangle_{fit}$ with respect to $\langle T \rangle_n$

$$f(E) = \frac{\sqrt{\pi}}{2\,M_a}\left[\mathrm{erf}\left(\frac{E - E_0}{\Delta E} + M_a\right) - \mathrm{erf}\left(\frac{E - E_0}{\Delta E} + M_a\right)\right]$$

$$M_a \ll 1$$

$$f(E) \propto \exp\left\{-\left(\frac{E - E_0}{\Delta E_{\mathrm{fit}}}\right)\right\} \Rightarrow \langle T_i \rangle_{\mathrm{fit}} = T_i + \frac{2}{3} m_i V_f^2$$

$$m_i = 2.5\ m_p,\ V_f = 3 \times 10^7\ \mathrm{cm/s},\ \frac{2}{3} m_i V_f^2 = 1.6\ \mathrm{keV}$$

- Effect of the flow is reduced because the peak in dn/d*t* is close to stagnation
- Effect of flow is stronger for implosions with large offset

For a typical low-adiabat cryogenic implosion with small offset $\langle T \rangle_{\text{fit}} \sim 95\% \langle T_i \rangle_n$

$\langle T_\text{i} \rangle_\text{n}$ keV	$\langle T \rangle_{\text{fit}}$ no flow	$\langle T \rangle_{\text{fit}}$ with flow
2.7	2.5	2.6

Ion temperature and yield are reduced because of hot-spot distortion growth

Shell at deceleration phase

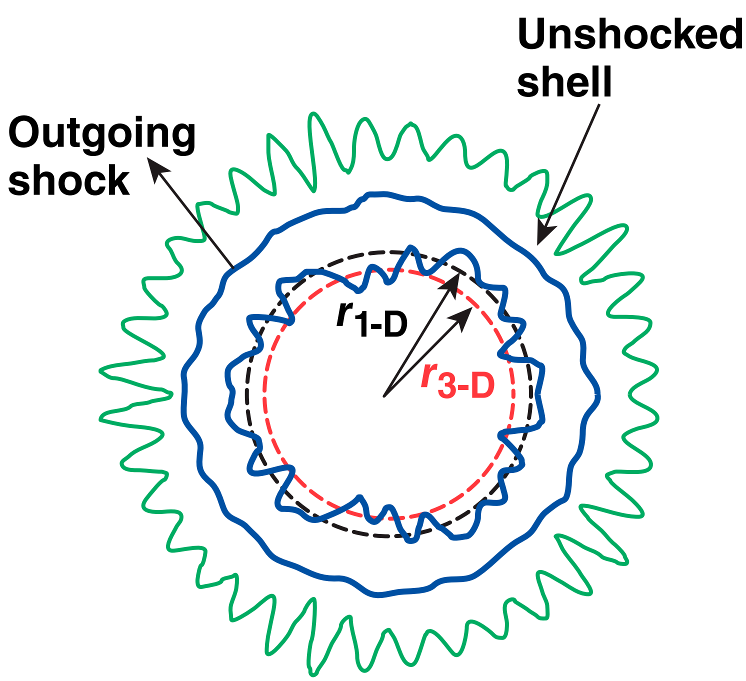

Effect of perturbations

(1) $V_{3\text{-D}} = \frac{4\pi}{3} r_{3\text{-D}}^3 < V_{1\text{-D}} = \frac{4\pi}{3} r_{1\text{-D}}^3$

$$r_{3\text{-D}} = r_{1\text{-D}} - \sqrt{\sum_{\ell} (w_{\ell} a_{\ell})^2} = r_{1\text{-D}} (1 - \xi)$$

Low–ℓ modes contribute less[1]

(2) Extra thermal conduction losses ⇒ lower T_e and T_i

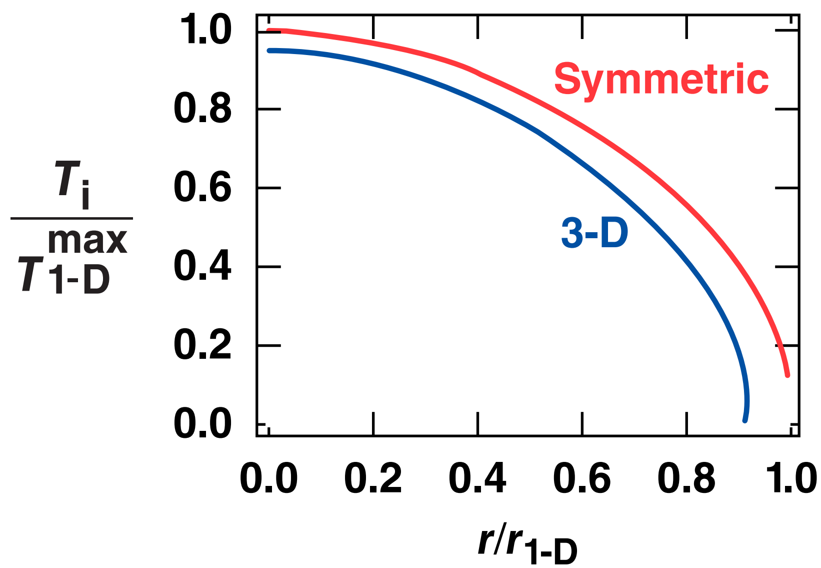

TC9024a

[1]P. Kishony and D. Shvarts, Phys. Plasmas 8, 4925 (2001).

For a typical low-adiabat cryogenic implosion with small offset $\langle T \rangle_{fit} \sim 95\% \langle T_i \rangle_n$

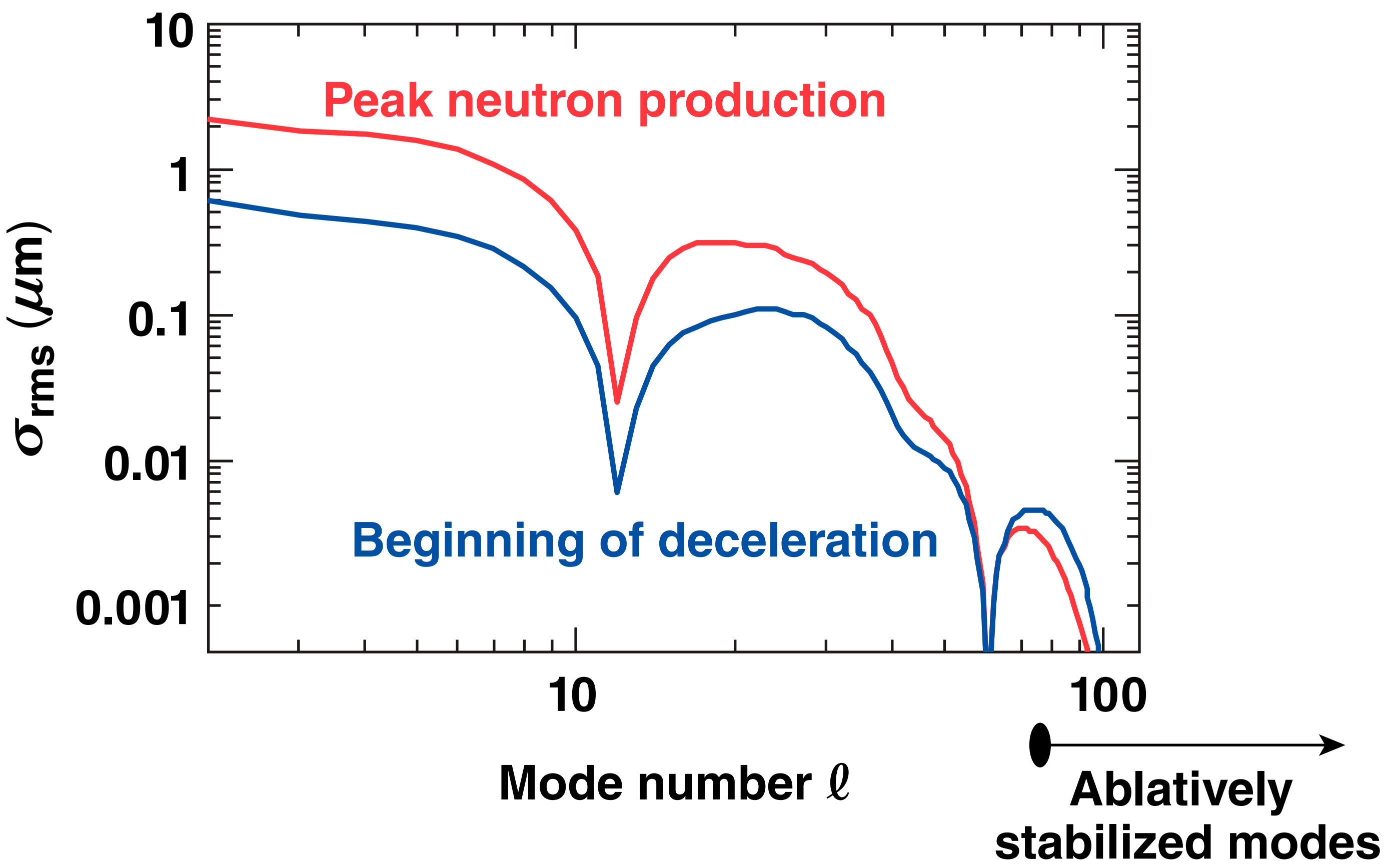

Moderate-size amplitude of $\ell = 2$ increases effective hot-spot region

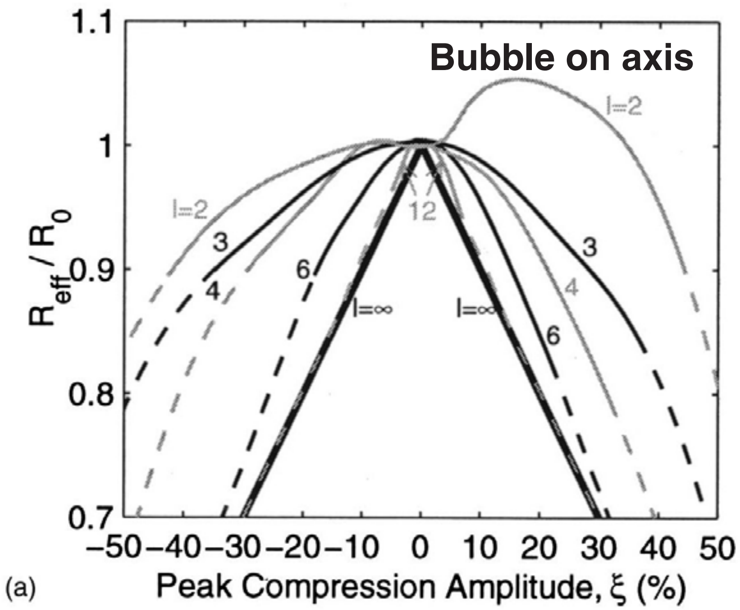

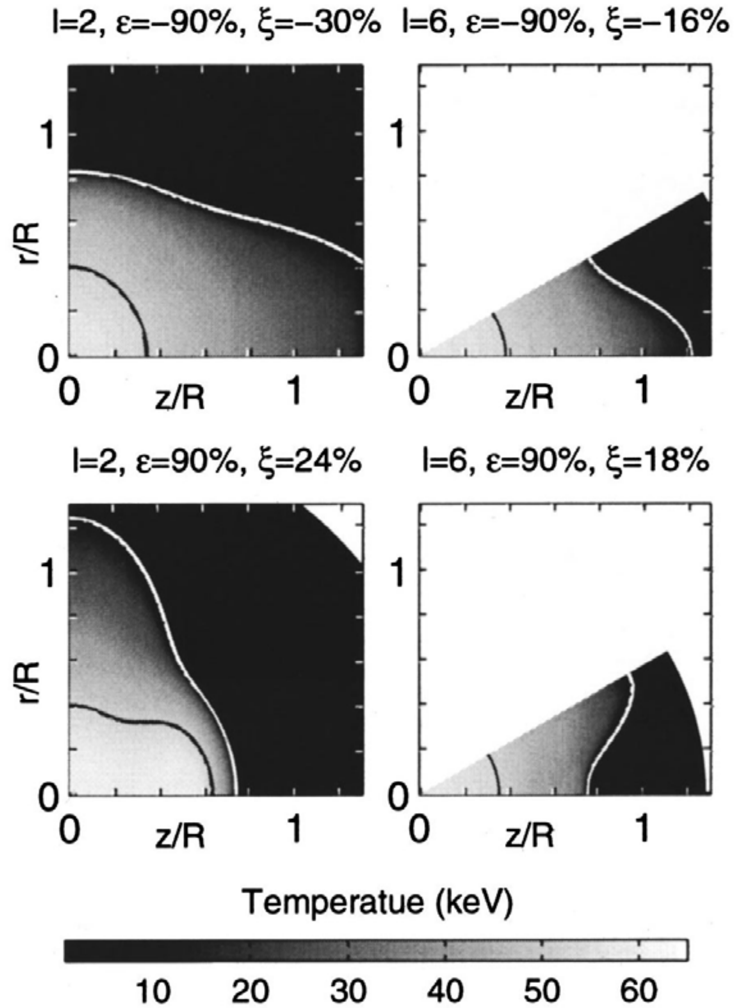

R. Kishony and D. Shvarts, Phys. Plasmas 8, 4925 (2001).

As the hot-spot deformations grow, effective volume reduction caused by short wavelengths compete with volume increase because of $\ell = 2$ growth

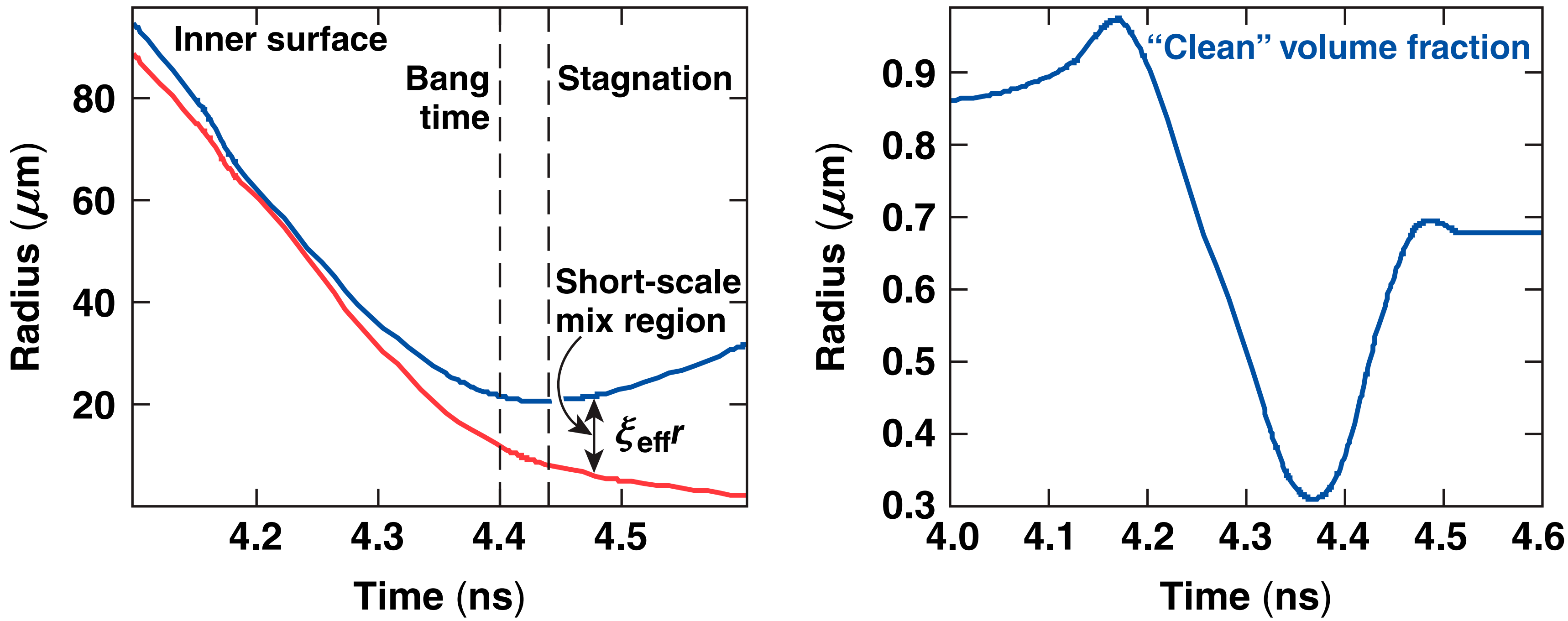

Increased hot-spot volume caused by $\ell = 2$ broadens the neutron rate